Application of modern 2-D and 3-D seismic-reflection techniques for uranium exploration in the Athabasca Basin[1]

Z. Hajnal, D.J. White, E. Takacs, I. Gyorfi, I.R. Annesley, G. Wood, C. O'Dowd, and G. Nimeck

Abstract: Seismic-reflection techniques have been applied in several studies over the last 20 years as a uranium-exploration tool within the Athabasca Basin and have been utilized to provide the larger structural context for known uranium deposits within the basin. At the crustal scale, deposits within the eastern Athabasca Basin are shown to be associated with deep-seated shear zones that originated during Trans-Hudson orogeny and have subsequently been reactivated during and subsequent to deposition of the basin-fill sandstones. Seismic properties of the Athabasca sandstones and underlying basement have been determined through in situ borehole measurements. Reflectivity within the sandstones is generally weak. Seismically recognizable signatures are primarily associated with variations in fracture density, porosity, and degree of silicification. The basement unconformity and regolith, a prime target of exploration, is widely imaged as it is characterized by variable but generally distinct reflectivity. Results from the McArthur River mine site suggest that the spatial coincidence of seismically imaged high-velocity zones and deep-seated faults that offset the unconformity may be a more broadly applicable exploration targeting tool. Three-dimensional (3-D) seismic imaging near existing ore zones can define the local structural controls on the mineralization and point the way to new targets, thus leading to more efficient exploration drilling programs. Furthermore, seismically generated structural maps of the unconformity and rock competence properties may play a significant role at the outset of mine planning.

Résumé : La sismique réflexion a été utilisée dans plusieurs études au cours des 20 dernières années en tant qu'outil d'exploration pour l'uranium dans le bassin de l'Athabasca; elle a aussi été utilisée pour fournir le contexte structural à plus grande échelle pour les gisements connus d'uranium à l'intérieur du bassin. À l'échelle de la croûte, il est montré que des gisements dans le bassin Athabasca oriental sont associés à des zones de cisaillement à grande profondeur qui ont pris naissance durant l'orogène trans-hudsonien et qui ont par la suite été réactivées durant et après la déposition des grès remplissant les bassins. Les propriétés sismiques des grès de l'Athabasca et du socle sous-jacent ont été déterminées par des mesures in situ dans des forages. La réflectivité est généralement faible dans les grès. Des signatures sismiques identifiables sont surtout associées à des variations de densité des fractures, de la porosité et du degré de silicification. La discordance entre le socle et le régolite, une cible de choix en exploration, est bien imagée en raison de sa caractérisation par une réflectivité variable mais généralement distincte. Les résultats provenant du site minier McArthur River suggèrent que la coïncidence spatiale de zones de grandes vitesses imagées par sismicité et de failles à grande profondeur qui décalent la discordance puissent être un outil plus largement applicable comme cible d'exploration. De l'imagerie sismique 3D à proximité des zones minéralisées existantes peut définir les contrôles structuraux locaux sur la minéralisation et indiquer de nouvelles cibles, menant ainsi à des programmes de forages d'exploration plus efficaces. De plus, des cartes de structure, générées par sismicité, de la discordance et des propriétés de compétence du roc pourraient jouer un rôle important dès le début d'une planification minière.

[Traduit par la Rédaction]

Received 19 September 20009. Accepted 22 February 2010. Published on the NRC Research Press Web site at cjes.nrc.ca on 9 June 2010.

Paper handled by Associate Editor R. Clowes.

Z. Hajnal[2] and E. Takacs. University of Saskatchewan, Department of Geological Sciences, 114 Science Place, Saskatoon, SK S7N 5E2, Canada.
D.J. White. Geological Survey of Canada, 615 Booth Street, Ottawa, ON K1A 0E9, Canada.
I. Gyorfi. Upstreamers Energy, str. Salcamilor 4A, Sfantu-Gheorgne 520052, Romania.
I.R. Annesley. JNR Resources, 204–315-22nd Street East, Saskatoon, SK S7K 0G6, Canada.
G. Wood and C. O'Dowd. Cameco Corporation, 2121-11th Street West, Saskatoon, SK S7M 1J3, Canada.
G. Nimeck. Areva Resources Canada Inc., 817-45th Street West, Saskatoon, SK S7K 3X5, Canada.

[1]This article is one of a series of papers published in this Special Issue on the theme *Lithoprobe — parameters, processes, and the evolution of a continent*.
[2]Corresponding author (e-mail: zoltan.hajnal@usask.ca).

Introduction

The Athabasca Basin has been actively explored for uranium for over a half century. Geophysical methods have played a major role in this region, as virtually all ore discoveries were based on drilling airborne-based or ground-based geophysical anomalies. Exploration activities have been mainly focused on the eastern margin of the basin where the shallow depth of the basement unconformity provides an accessible target for potential field or electrical methods in search of unconformity-based deposits. More recently, the migration of exploration into the deeper parts of the basin has fostered an interest in geophysical methods capable of probing to greater depths. This has resulted in a new interest in utilizing seismic methods within the basin.

Until recently, seismic methods had not been extensively tested in the basin. Reconnaissance refraction studies (Hobson and MacAuley 1969; Overton 1977) successfully mapped broad-scale depth variations of the sandstone-basement contact throughout the basin, producing maps that still provide useful background information for exploration. Initial attempts at using seismic-reflection methods within the basin resulted in limited success (Scott 1983; Fouques et al. 1986). The first successful test of high-resolution seismic imaging within the basin was conducted in 1994 by Lithoprobe and a consortium of mining companies (Hajnal et al. 1997). Based on this success, there have been a number of subsequent research and commercial seismic surveys, including Shea Creek in 1997, EXTECH-IV McArthur River in 2004, Russell and Moore Lake surveys in 2004 and 2005, and Midwest NE and Millenium 3-D surveys in 2007. The objectives of these studies included (1) defining the subsurface stratigraphy and structure of the sedimentary rocks within the basin, (2) providing a detailed image of the basement unconformity that appears to host most of the ore deposits, (3) defining the structural framework that controls the deposits, and (4) developing more effective methods to characterize the variable nature of the unconformity and alteration zones associated with the ore deposits.

In this paper, we briefly describe the seismically derived geological framework that provides context for uranium deposits in the Athabasca Basin. This is followed by a summary of log-based seismic properties for the sedimentary rocks and underlying basement. The initial Lithoprobe-industry study is presented, followed by case histories of industry-sponsored studies from Shea Creek and McArthur River from the western and eastern basins, respectively. Finally, we discuss how seismic imaging has been useful in mapping both major regional and mine-scale (ore-related) structures and generally assess the effectiveness and limitations of seismic-reflection techniques as applied in these studies.

Regional geology

The world's highest grade uranium deposits are the unconformity-type deposits of the Mesoproterozoic Athabasca Basin of northern Saskatchewan and Alberta, Canada (Fig. 1). The Athabasca Basin (Figs. 2, 3*a*) comprises an undeformed clastic sequence that unconformably overlies the highly deformed and metamorphosed rocks of the Rae and Hearne subprovinces of the western Churchill Province. The

Fig. 1. Simplified geology map showing the location of the Athabasca Basin relative to the major Precambrian provinces in North America.

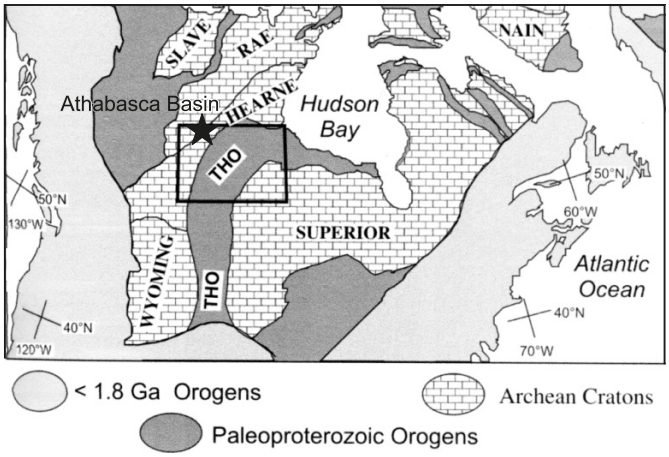

Hearne subprovince beneath the eastern part of the basin is divided into the Mudjatik Domain, Wollaston Domain, and the Wollaston–Mudjatik Transition Zone. These domains comprise Archean granitic to granodioritic to tonalitic orthogneisses that are stratigraphically overlain by and structurally intercalated with the Paleoproterozoic Wollaston Group supracrustal package (Annesley et al. 1997, 1999, 2001, 2005). The basal Wollaston Group gneiss units wrap around the Archean basement domes such that the overlying Wollaston Group strata young outwards. The lower Wollaston Group within the western Wollaston domain is mainly composed of a basal pelitic gneiss unit, commonly graphitic in nature, and an overlying sequence of psammitic to psammopelitic gneisses intercalated with calc-silicate gneisses and meta-quartzites (Annesley et al. 2005). This supracrustal package has been intruded by syn- to post-peak thermal metamorphic granitic pegmatites and leucogranites of Hudsonian age. Hydrothermal albitization and calc-silicate alteration of the basement rocks occurs locally and is interpreted to be related to high-temperature retrograde metamorphism–metasomatism and late-tectonic Hudsonian intrusions.

Intense deformation and metamorphism of the basement rocks resulted from the continent–continent collision of the Trans-Hudson Orogen (ca. 1.8 Ga), which led to the development of the Wollaston fold–thrust belt. The structural framework within the eastern Athabasca Basin (Tran et al. 2003), as depicted schematically in Fig. 3*b*, shows all of the major structures verging toward the NW to WNW. Similarly, work by Portella and Annesley (2000) and Annesley et al. (2003) shows comparable NW- to WNW-verging structures but indicate SE- to SSE-verging structures further to the southeast within the THO.

The basement geology of the western Athabasca Basin is not as well established. West of the Snowbird Tectonic Zone (Fig. 2), and mainly within the region of interest, the crystalline basement comprises part of the Archean Rae Province, which is subdivided into the Tanto, Lloyd, and Clearwater domains (Card et al. 2007). The younger Paleoproterozoic Clearwater Domain is juxtaposed between the western and eastern Lloyd domains. This laterally limited domain is recognized through its distinct high-positive-magnetic and low-

Fig. 2. Total-field aeromagnetic map for the Athabasca Basin region, modified from Card et al. (2007). It illustrates the high correlation between the magnetic signatures and the major tectono-stratigraphic domains of the basement, structures, and fault systems in the region. RL, location of the Rumple Lake borehole. Within the eastern Athabasca Basin, the major ore deposits are located on a northeast trend, mainly within the boundary zone between the western Wollaston Domain and the Mudjatik Domain. Square with white internal colour, 2-D seismic surveys up to 2010; square with yellow internal colour, 3-D seismic surveys to date; northwest–southeast heavy black line is the approximate location of the geologic cross section of Fig. 3*a*; S2B, Lithoprobe deep seismic profile across the western Trans-Hudson Orogen (THO; see Fig. 4); S2D, Lithoprobe-industry high-resolution seismic profile (see Fig. 10).

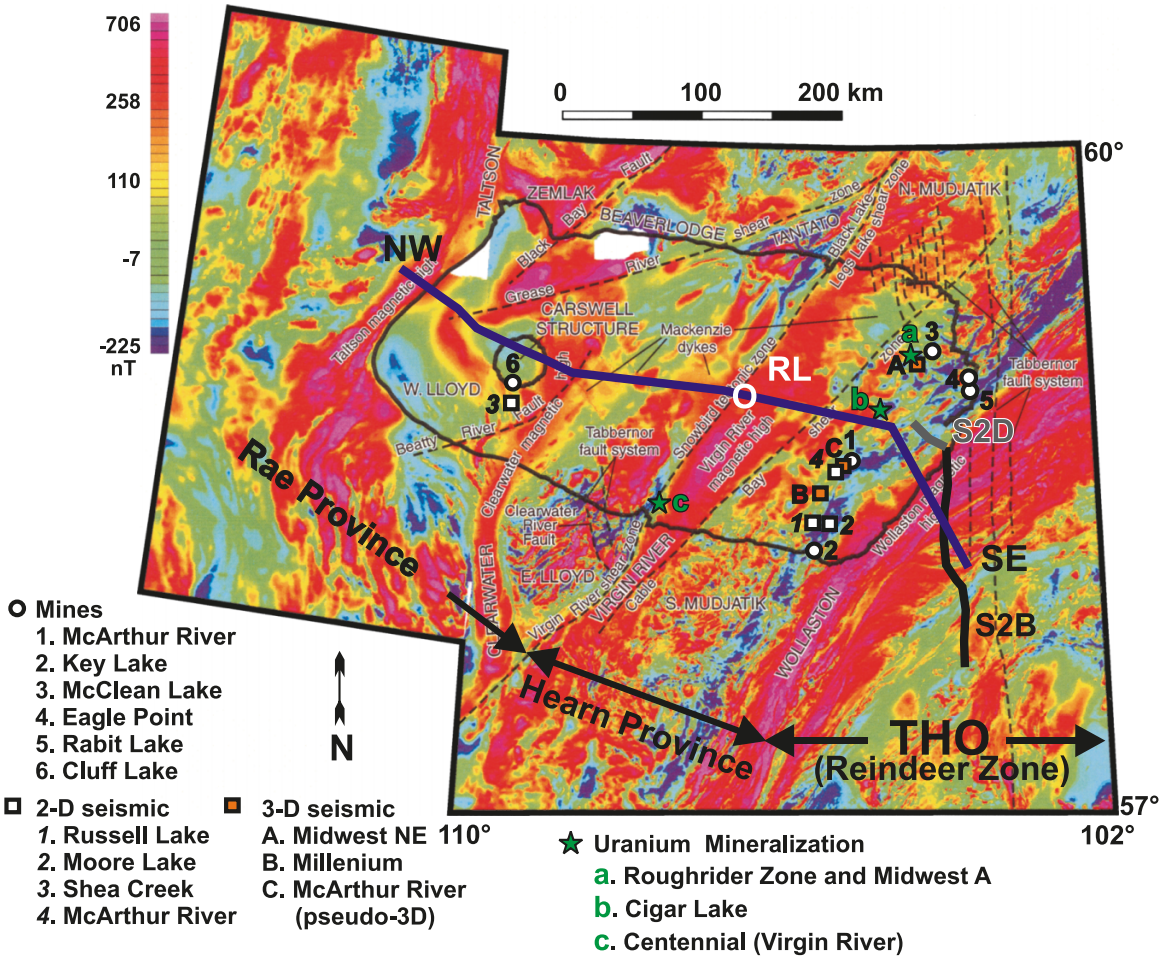

gravity signatures. The rocks of the domain are weakly deformed equigranular K-feldspar-phyric biotite granites that intruded older granitic gneiss.

The Mesoproterozoic sedimentary rocks that form the basin-fill (Fig. 3*a*) reside beneath a mantle of Quaternary till deposits of variable thickness (0–90 m; Schreiner 1983) that is mainly composed of poorly sorted sand and gravel with abundant boulders. The basin fill is flat-lying, reaching a maximum thickness of ~1800 m, and comprises red, fluviatile, quartz-dominated siliciclastic sequences of fluvial conglomerate, sandstone, and mudstone resting on peneplaned tectonometamorphic complexes. It is geologically subdivided into seven lithostratigraphic units (Fig. 3*a*). At the unconformity, a variable thickness (0~70 m) of red hematitic regolith grades downwards through green, chlorite-altered rock into fresh basement rocks of variable composition. The regolith is interpreted as a result of regional paleoweathering that has been overprinted by diagenetic bleaching and additional hematite alterations (Jefferson et al. 2007). The sandstones and underlying basement rocks have been subjected to several episodes of brittle deformation, including the brittle reactivation of older ductile shear zones.

To date, most of the major unconformity-type uranium deposits and mines in the Athabasca Basin are located within the eastern portion (Fig. 2). The deposits generally occur near reactivated Trans-Hudsonian crustal shear zones (Annesley and Madore 2002; Annesley et al. 2005; Jefferson et al. 2007 and references therein). Reactivation of many of these basement structures brackets the period of deposition of the basin-fill sediments, and thus these structures constitute important structural controls on the ore deposits. The intersection of the sub-Athabasca unconformity with these basement-rooted faults provided the structural–geochemical traps for deposition of large high-grade uranium deposits during hydrothermal circulation.

Regional seismic-reflection studies

Seismic-reflection studies in northwestern Saskatchewan

Fig. 3. (*a*) A northwest–southeast lithostratigraphic cross section of the basin based on borehole and geophysical data (after Ramaekers et al. (2007). (*b*) A diagrammatic cross section of the basement east of the Virgin River shear zone (Fig. 2), adapted from Tran et al. (2003).

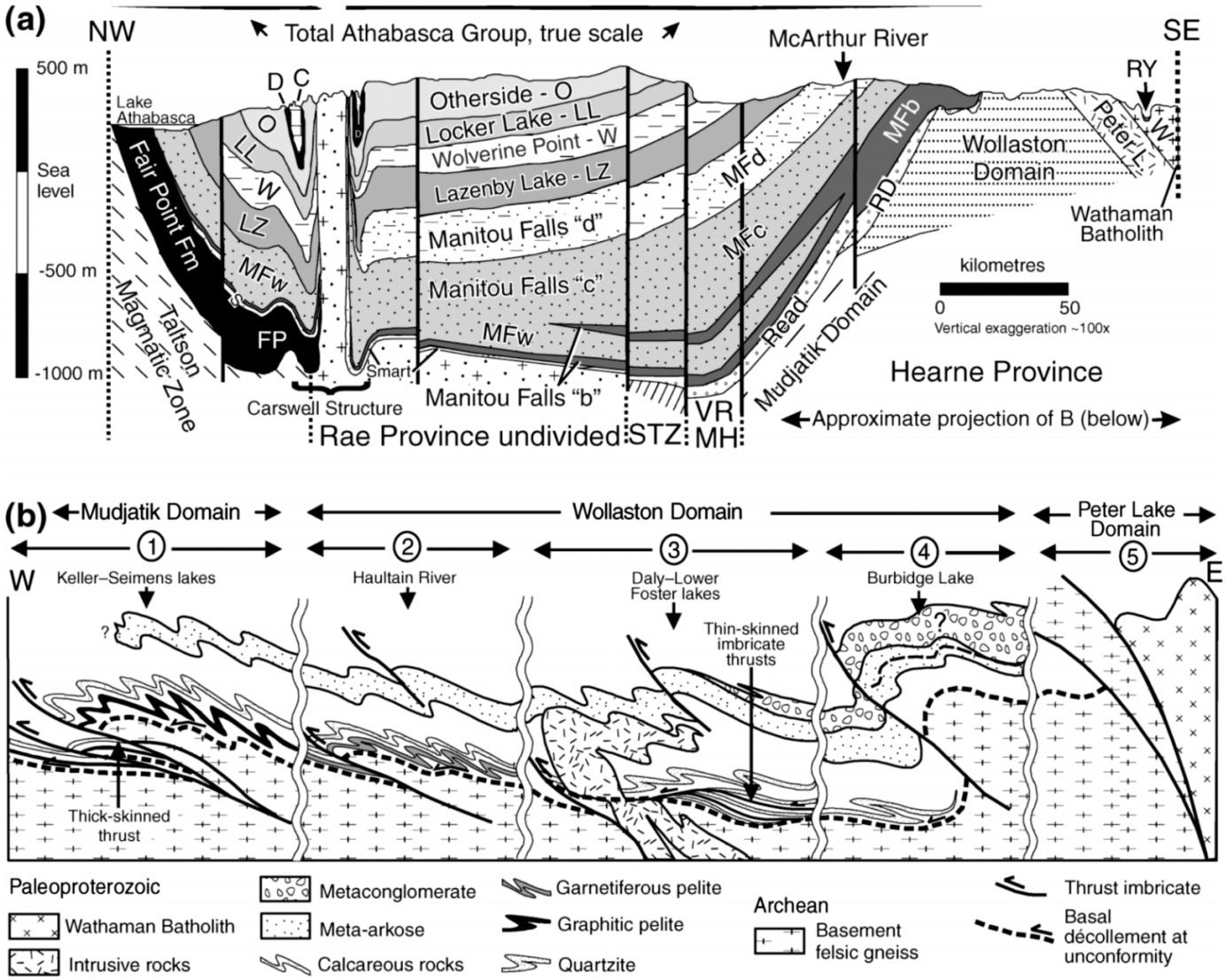

were conducted as part of the Lithoprobe Trans-Hudson Orogen Transect (THOT) in an attempt to image the crustal architecture of the western margin of the orogen (Hajnal et al. 1996; Hajnal et al. 2005). Seismic-reflection profile S2B (Fig. 4) extended from the exposed shield to ~32 km into the Athabasca Basin. Detailed interpretation of this profile can be found in Hajnal et al. (2005) and references therein. More recently, two short deep-sounding seismic surveys were acquired near the MacArthur River mine as part of the EXTECH-IV project (Hajnal et al. 2007). The Lithoprobe and shorter EXTECH-IV surveys traverse comparable segments of the western margin, separated by ~100 km along strike. Comparison of these profiles allows correlation of structures within the mining camp to those of the regional crustal structure. Regional crustal structures appear to have significant relevance to the development and reactivation–remobilization of economic uranium mineralization in the Athabasca Basin.

An interpretation of Lithoprobe line S2B (based on Hajnal et al. 2005) for the shallow and middle crust is shown in Fig. 4. West-dipping structures that characterize the southeastern side of the profile are replaced by east-dipping structures to the northwest. This characteristic pattern was interpreted by Hajnal et al. (2005) as collision-related east-vergent thrusts and west-vergent backthrusts. A prominent, laterally continuous reflector (BR, Wollaston Lake reflector; e.g., Mandler and Clowes 1997) deepens westward from a minimum depth of ~6–12 km at the northwest end of the profile. Comparable features are also recognized on the MacArthur River sections (Fig. 5) ~100 km southwest of S2B and by several other recent seismic studies within the eastern portion of the Athabasca Basin (Hajnal et al. 2009). Reprocessing of the uppermost part of line S2B suggests that the Wollaston Lake reflector is young with respect to the overall structural framework. It may be associated with 1270 Ma Mackenzie sills (e.g., Mandler and Clowes 1997) or, alternatively, a low-angle basal detachment zone associated with late extension (Gyorfi 2006). The east-dipping P2 fault on line B (Fig. 5), which is associated with the ore zone at MacArthur River, is one of the reactivated back-

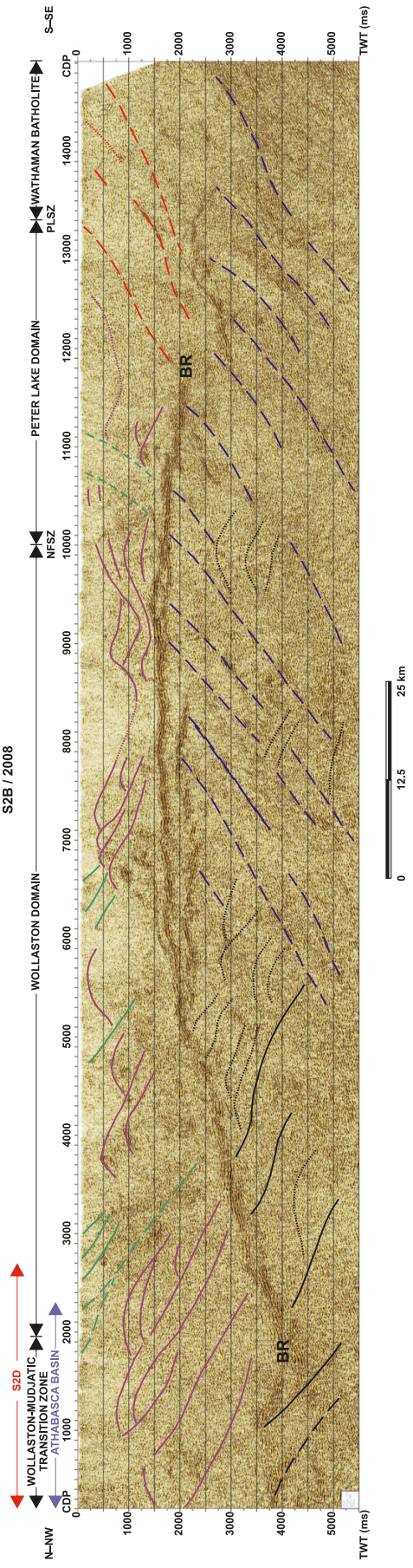

Fig. 4. The first 5.0 s (two-way traveltime, TWT) of line S2B (Fig. 2) of the Lithoprobe deep seismic section, Trans-Hudson Orogen (THO; Hajnal et al. 2005). BR, Bright reflector (Wollaston Lake reflector); NFSZ, Needle Falls Shear Zone; PLSZ, Parker Lake Shear Zone. The dark (black and violet) coloured lines represent crustal structures recognized through the original Lithoprobe investigation. The bright (red and green) coloured lines represent structures discovered after recent reprocessing of the upper portion of the seismic data. Fault systems are recognized as close as ~500 m from the surface. Currently, some of these structures are a part of active exploration.

thrusts that acted as a conduit for the migration of the mineralized fluids. Early mapping of these significant subsurface tectonic elements can expand exploration target zones in depth far beyond recognition by any other indirect techniques.

High-resolution seismic studies

Acoustic properties

Acoustic properties of the Athabasca Basin rocks have been investigated by geophysical logging surveys, laboratory measurements on core samples, measured mineral properties, and results of vertical seismic profiling (Hajnal et al. 1983; Mwenifumbo et al. 2002; Mwenifumbo et al. 2004; White et al. 2007). An example of a sonic log and calculated synthetic seismic response for a drill hole in the MacArthur River camp is shown in Fig. 6*a*. Mean values of sandstone, silicified sandstone, and basement rocks derived from down-hole logging (summarized in Table 1) illustrate that the contacts between certain rock units can have significant seismic contrasts. To compensate for the limited information on basement rocks, estimates were also derived by considering mineral compositions using known mineral properties (Table 2). Comparison of these values with those from log measurements in basement rocks where alteration is present shows that alteration lowers the velocities significantly. Figure 6*b* depicts a summary of reflection coefficient values for the variety of expected geological conditions in the neighborhood of the unconformity and within the sandstone column.

The basin-fill sediments have relatively uniform bulk mineralogical composition, thus in general weak reflectivity. There are no distinct acoustic properties associated with the geologically defined stratigraphic units (Fig. 3*a*). However, local variations in density, porosity (fracture), and volume fraction in clay can vary compressional wave velocity (V_P) (White et al. 2007). Highly silicified zones also have higher acoustic impedances than unsilicified sandstones and therefore represent potential seismic reflectors within the basin-fill (Mwenifumbo et al. 2004). Internal reflectivity of the sandstones will generally be controlled by porosity variations. As shown in Fig. 6*b* (cases 1–3), reflectivity should generally be weak ($R < 0.05$) except where zones of contrasting porosity are juxtaposed, for example where fracture zones ($R = -0.08$; very local effect) and bedding-parallel silicification ($R = 0.11$) occur.

The acoustic properties across the unconformity will generally be variable, as it is characterized by complex, laterally variable chemical alteration. As can be seen in Fig. 6*b*, the resultant reflection coefficients range from –0.1 to 0.31 for cases 4–8. The sandstone-basement contact should generally be a very strong reflector ($R = 0.27$–0.31, case 4), but the reflection strength will be reduced if the overlying sandstone is silicified ($R = 0.11$–0.16, case 5). The reflection strength will also be reduced if a pronounced regolith is present (case 8). Extensive fracturing at the base of the sandstone (case 7) will result in reflections from the top ($R = -0.11$) and bottom (basement, $R = 0.25$) of the resultant low-velocity zone. The presence of a basal conglomerate layer (case 6) may also result in a double reflection.

Examples of observed variable reflectivity at the uncon-

Fig. 5. Line B from McArthur River includes the version from Hajnal et al. 2007 showing the upper half of the section to highlight the P2 fault and the BR. UC, unconformity.

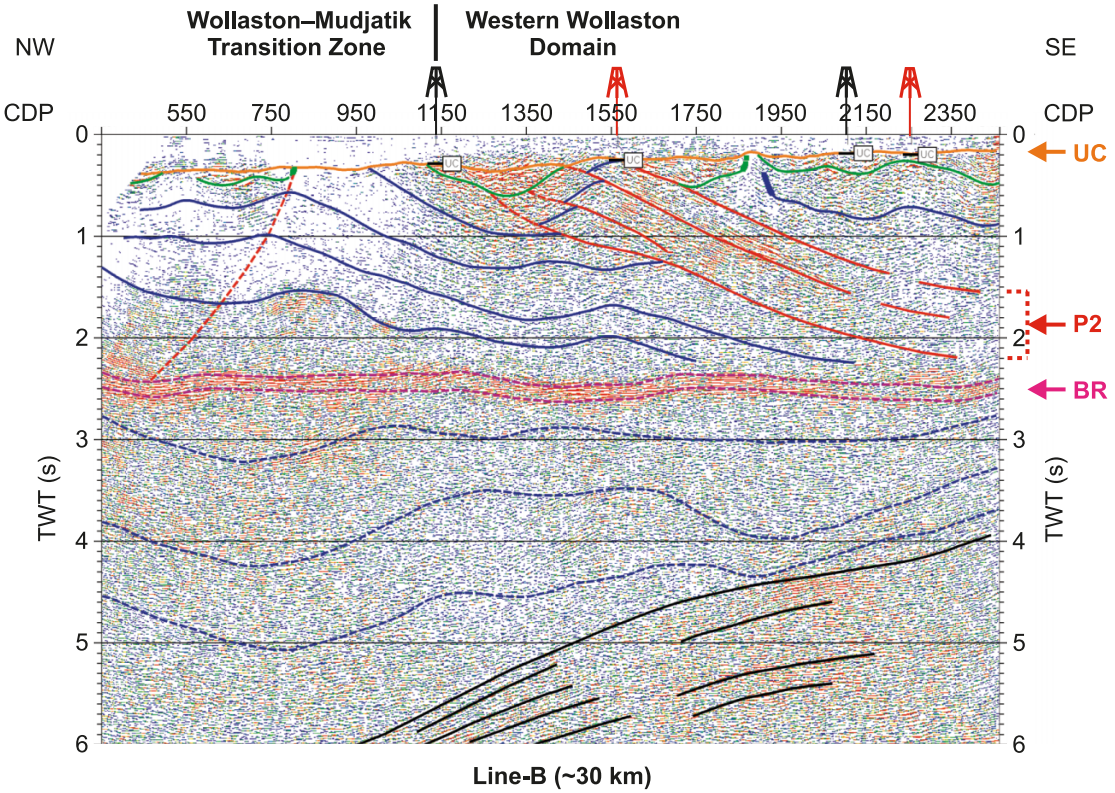

formity are shown in Fig. 7 and are related to particular interpreted geological scenarios. Direct contact between unaltered sandstone and basement rocks ($R = \sim 0.30$) generates distinct reflections (Fig. 7*a*). Silicified sandstone in contact with moderately altered basement still represents a significant contrast ($R = \sim 0.15$; Fig. 7*b*) and an observable unconformity reflection; whereas for $R = 0.08$ or lower contrasts, the seismic signal falls below the background noise (Fig. 7*c*). These examples are taken from the MacArthur River high-resolution profile 12 that is presented later in detail.

Data acquisition and processing

Since the initial Lithoprobe–industry high-resolution survey conducted in 1994, there have been a number of subsequent surveys including EXTECH-IV McArthur River (Gyorfi et al. 2007; White et al. 2007), Shea Creek, Millennium 3-D (Wood et al. 2009), Moore Lakes and Russell Lake in 2004 and 2005. The parameters used for data acquisition amongst these various high-resolution surveys are summarized in Table 3 and compared with typical regional acquisition parameters. Data acquisition for all of the seismic surveys was contracted through commercial seismic companies, assuring that the latest in instrumentation was used. From 1994 to 2001, the number of accessible recording channels increased from 450 to over 1000. During the earlier surveys, groups of 6–8 mechanical geophones were typically deployed in a linear array at each station. However, this proved cumbersome given the small geophone group station spacing and single geophone deployment at recording stations is now commonplace. This started with the EXTECH-IV survey in 2004 where prototype I/O Vectorseis three-component silicon-based micro-electronic – mechanical systems (MEMS) accelerometers were deployed for the first time in a mineral exploration survey. With the exception of the Millennium 3-D seismic survey, Vibroseis energy sources have been used exclusively. Historically, implementation of explosive sources was attempted in the basin, but they generated only marginal results owing to placement of the charges at very shallow depth in unconsolidated material. A VIBSIST-1000 (Cosma and Enescu 2001; Yordkayhun et al. 2009) energy source was tested in the Millennium 3-D survey. The source generated reliable data (Wood et al. 2009) but required a large number of impacts per source point and consequently more time per shot than the Vibroseis.

In general, the observed field data from the different surveys are variable in quality. A common source of coherent noise (scattering and multiples) in most surveys is the large acoustic impedance differences that occur at the interface between the glacial till and underlying sandstone. Average acoustic velocity within the till is ~ 1000 m/s with variations of ±20%, as compared with ~ 4000 m/s in the underlying sandstone. When the seismic arrivals of interest occur at ~ 0.300 s (or ~ 500 m) or less, the coherent noise overwhelms the primary seismic signals of interest resulting in marginal signal-to-noise (S/N) levels (Fig. 8). In the deeper part of the basin, the arrival times of the noise are partially separated (Fig. 9) from the later incoming signals, thereby

Fig. 6. (*a*) Seismic properties for drill hole MAC257 from McArthur River. From left to right are sonic velocities from logging, calculated acoustic impedance from sonic and density logs, calculated reflection coefficient series, and synthetic traces determined by convolving the reflectivity series with the source wavelet shown at the top of the figure. The unconformity, fractures (Fr) and tops of the regolith and unaltered basement are labeled. (*b*) Summary of predicted reflection coefficients for various geological scenarios. See text for details. Overlapping arrows are designed to indicate the expected variability in reflection coefficients for the associated geological scenario described in the text. Two arrows for a given scenario indicate that two distinct reflections may occur. ss, sandstone; fr, fractured; sil, silicified; bsmt, basement; fangl, fanglomerate.

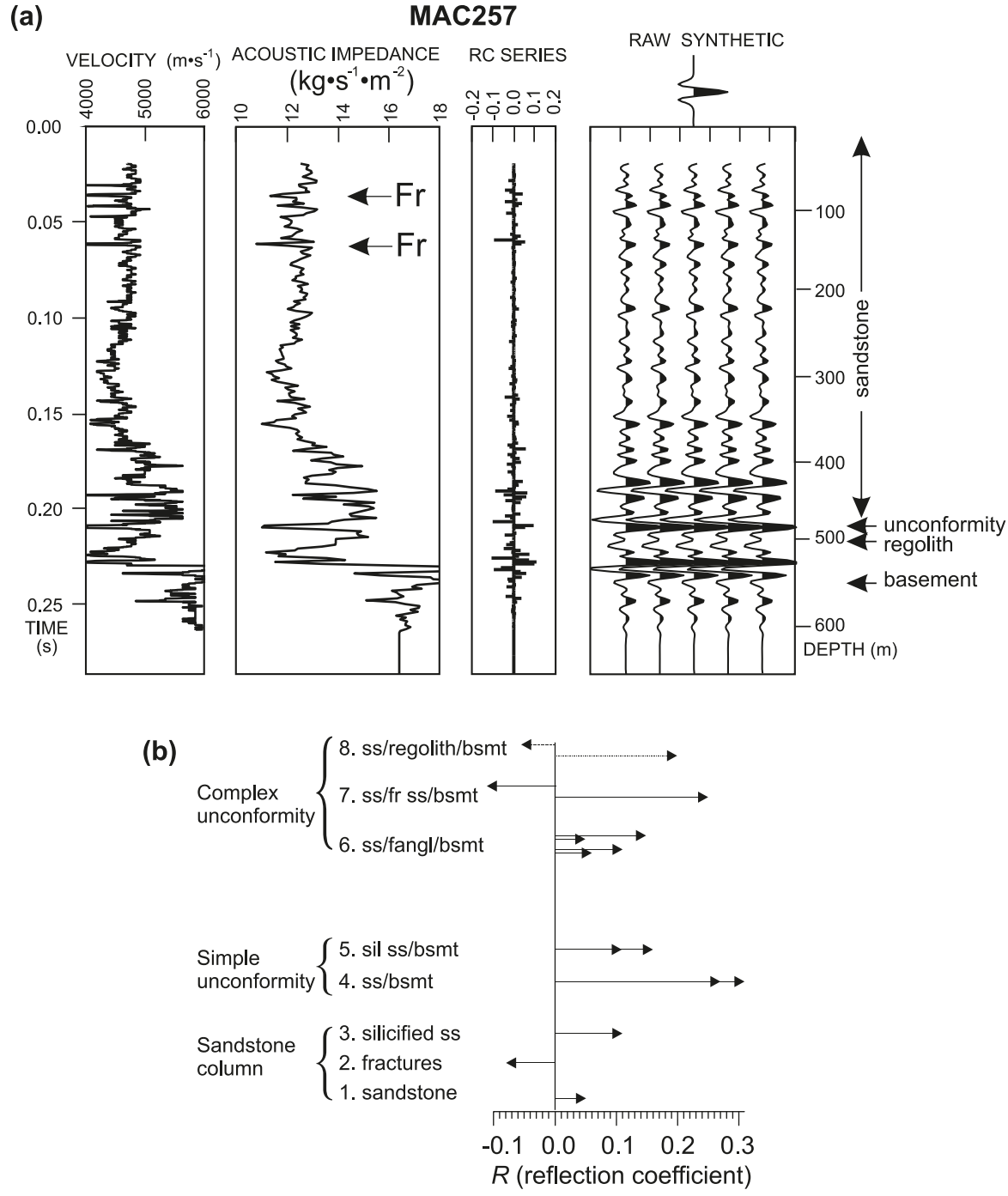

resulting in visibly higher S/N levels. Suppression of the various coherent noise patterns (Fig. 8) can be challenging. A representative list of processing procedures for the high-resolution seismic data is compiled in Table 4. Minor variations from this list occur to adapt to localized near-surface variations.

Exploration-related experiments

Lithoprobe line S2D

In collaboration with the mining industry, the 1994 phase of the Lithoprobe program acquired a high-resolution profile (S2D, Fig. 2) along the Athabasca Basin segment of regional

Table 1. Mean values for sandstone, silicified sandstone, and basement rocks from in situ down-hole geophysical logging from Mwenifumbo et al. (2004).

Lithological unit	Mean compressional wave velocity, V_P (km·s^{-1})	Mean density (g·cm^{-3})	Acoustic impedance ($\times 10^6$ kg·s^{-1}·m^{-2})
Sandstone 1	4.29	2.14	9.7
Sandstone 2	4.72	2.30	10.9
Silicified sandstone	5.43	2.44	13.3
Basement	5.15	2.53	13.8
Basal conglomerate	5.66 (0.18)	2.59 (0.04)	14.7

Note: Standard deviations (in parentheses) are provided when available. Table is from White et al. (2007).

Table 2. Physical properties of basement rocks estimated from fractional mineral compositions.

	Mean compressional wave velocity, V_P (km·s^{-1})	Mean density (g·cm^{-3})	Acoustic impedance ($\times 10^6$ kg·s^{-1}·m^{-2})
Quartzite: 100% quartz	6.22	2.65	16.5
Psammitic gneiss: 20% sillimanite	6.69	2.77	18.5
Pelitic gneiss: 3% garnet, 15% biotite	6.14	2.75	16.9
Pelitic gneiss: 10% garnet, 25% biotite	6.17	2.89	17.8

Note: The gneisses are composed of the indicated mineral fractions with quartz constituting the remainder. V_p estimates were obtained using a simple time-average equation (Sheriff and Geldart 2006, p. 117). Table is from White et al. (2007).

Fig. 7. Observed seismic images of the unconformity at locations of different acoustic contrast. The images are from the EXTECH-IV high-resolution seismic survey at MacArthur River: (*a*) normal, direct contact between unaltered sandstone and fresh basement; (*b*) silicified ss, silicified sandstone overlies partially altered basement; (*c*) ss/bsmt silicified, both sandstone and basement altered, only minimal acoustic contrast. S1, intra-sandstone reflection; S2, unconformity-related reflection; *F*, fault.

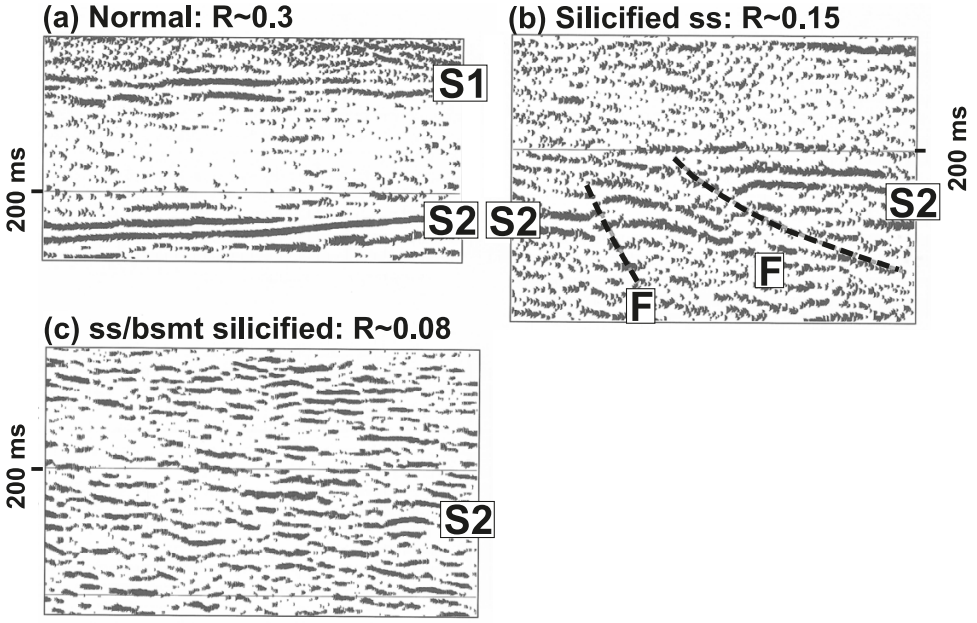

line S2B. The objective was to image the unconformity and the underlying basement structures, two fundamental requirements of any exploration program in the basin. As can be seen in Fig. 10, the unconformity is well imaged. The depth of the unconformity is mapped with an accuracy of ±5% or better when compared with borehole information (Hajnal et al. 1997). Numerous steeply dipping, unconformity–offsetting faults were recognized. The east end of the line located outside of the basin margin illustrated that the exposed basement can be reflective when pelitic gneisses and Archean volcanic rocks are in contact.

Several structural systems are also recognized within the basement. On the east side, several gently east-dipping thrust sheets reactivated the earlier ductile altered zone, leading to brittle deformation and the formation of west-dipping fault blocks. These faults are attributed to the Tabbernor fault system (Fig. 2). East of common-midpoint (CDP) 6000, the structural architecture changes across a

Table 3. Two-dimensional (2-D) and three-dimensional (3-D) data acquisition parameters.

	2-D high resolution	2-D regional	3-D high resolution
Recording instrument	IO system two 24-bit telemetry, with noise burst edit and diversity stack	IO system two 24-bit telemetry, with noise burst edit and diversity stack	IO system two 24-bit telemetry, with noise burst edit and diversity stack, and VectorSeis remote seismic recorders
Source type	IVI Y-2400 22 000 kg Vibroseis buggy, 47 700 lbs peak force per unit	IVI Y-2400 22 000 kg Vibroseis buggies, 47 700 lbs peak force per unit	IVI Y-2400 22 000 kg Vibroseis buggy, 47 700 lbs peak force per unit
Number of vibes	1	4	1
Vibration point (VP) interval (m)	15	50, 25 m for 3 km at line ends	15
Sweep frequencies (Hz)	30–180 nonlinear (3 dB/octave) upsweep	10–84 linear upsweep	30–180 nonlinear (3 dB/octave) upsweep
Number of sweeps per VP	6	6 (4 vibes) or 10 (3 vibes)	6
Sweep length (s)	12	28	12
Record length (correlated) (s)	6	18	6
Geophone group interval (m)	5	25	30
Geophones per group	1	6 over 25 m	1
Geophone type	VectorSeis	10 Hz	VectorSeis
Sample interval (ms)	1	1	1
Number of recording channels	541 vertical component	960 vertical component	1080 detectors/patch

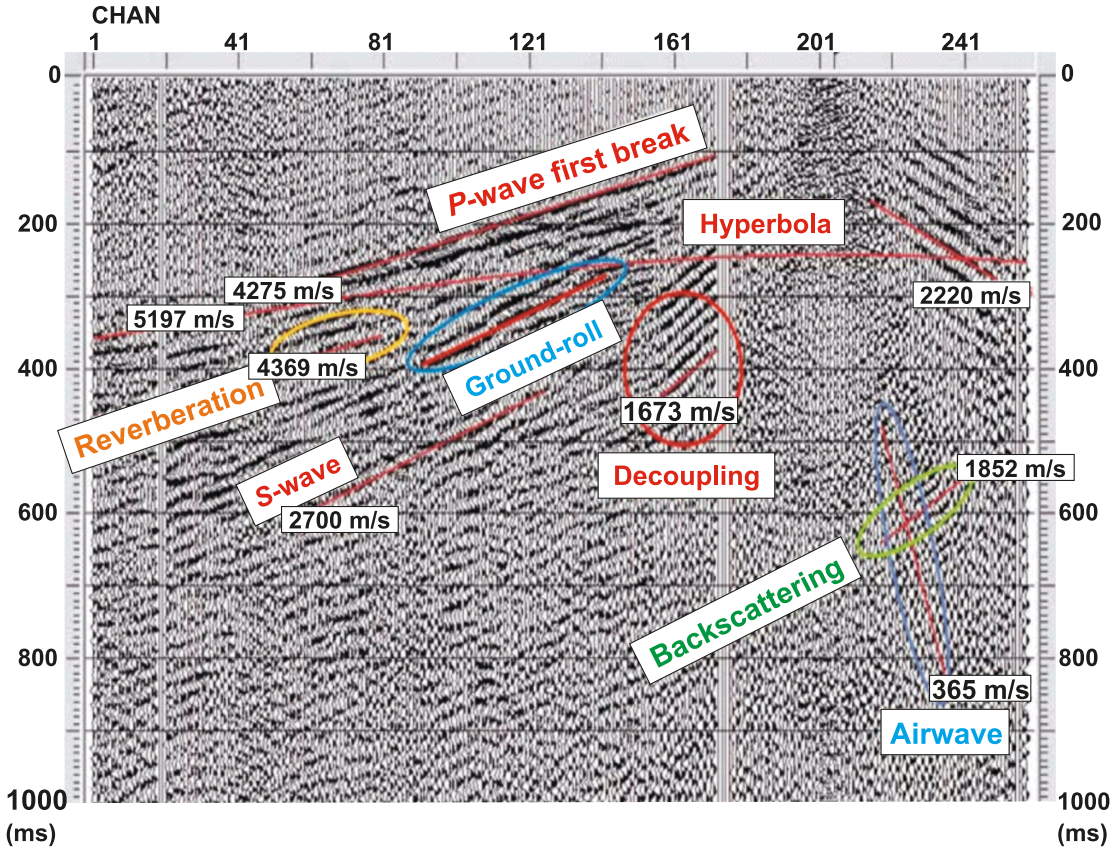

Fig. 8. A raw field record from the McArthur River survey. The reflection hyperbola for the unconformity reflection is expected at ~250 ms arrival time. It is not visible due to the overwhelming amplitude of the strong source-generated coherent noise.

prominent east-dipping fracture zone that can be traced from the unconformity to ~9000 m depth. This transition is inferred to be the eastern boundary of the Wollaston–Mudjatik Transition Zone. The unconformity is highly anomalous and fragmented by faults, which penetrate into the overlying sandstone (Fig. 10*b*). The Midwest, Midwest-A, and the more recent Roughrider uranium ore deposits are located a few kilometres further along the projection of this complex

Fig. 9. Shot gather from the Shea Creek survey. The reflection events are visible on this field record partly because the unconformity arrivals are later at the Shea Creek site, occurring later on the field record where coherent noise trains are not as prominent. In addition, the Vibroseis sweep started at a relatively high frequency (50 Hz) during data acquisition, thereby reducing the amount of low-frequency source-generated noise. UC, unconformity.

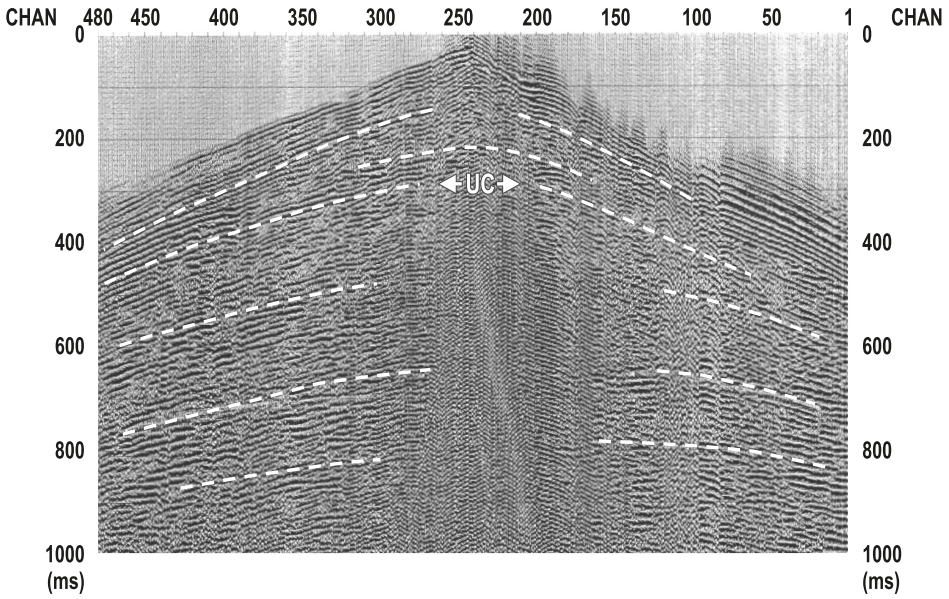

Table 4. Representative list of processing procedures for the high-resolution seismic data.

Order	Processing steps
1	Editing and geometry assignment
2	Refraction statics (generalized linear inversion method)
3	Time variant predictive deconvolution
4	Frequency–wavenumber (*f*–*k*) filtering (1)
5	Radon (*tau*-*p*) filtering
6	Muting
7	Velocity analysis (1)
8	Residual statics (1)
9	Frequency–wavenumber (*f*–*k*) filtering (2)
10	Velocity analysis (2)
11	Residual statics (2)
12	Normal moveout (NMO) correction
13	Dip moveout (DMO) correction
14	Velocity analysis (3)
15	Residual statics (3)
16	Common-midpoint (CDP) stacking
17	Frequency–offset (*F*–*X*) deconvolution
18	Post-stack Kirchoff time migration

basement structure; and all three deposits are associated with prominent basement shear zones.

Shea Creek

Background geology

The Shea Creek and the Cluff Lake uranium deposits lie within the western Lloyd Domain in the vicinity of the Clearwater magnetic high (Figs. 2, 11). In the Shea creek region, the basement comprises a granulite-facies metamorphic succession of upper felsic quartzofeldspathic gneiss, a middle aluminous metasedimentary (metapelites and garnetites) unit, and lower felsic gneiss. The middle unit contains the Saskatoon Lake Conductor, which provided the targets for the first drilling program and subsequent uranium discovery. The Cluff Lake mine is located at the southern margin of the basement core of the Carswell structure (Fig. 2). This nearly circular structure is ~39 km in diameter and contains an 18 km wide basement uplift in its core and an outer annulus of the uppermost formations of the Athabasca Group. It has been interpreted as a meteorite impact structure (Pagel and Svab 1985; Grieve and Masaitis 1994) with the uplift of the central core being responsible for transporting the U deposits to the near-surface (Baudemont and Fedorowich 1996). Borehole logs from the Shea Creek area (Fig. 12) show a thin layer of glacial till lying above a sandstone succession consisting of Locer Lake, Wolverine Point, Lazenby, and Manitou Falls D and C formations. The EXTECH-IV program (see later in the text) has subsequently provided a comprehensive description of the lithostratigraphic properties of the Athabasca Group sandstone sequences (Ramaekers et al. 2007; Rainbird et al. 2007).

The seismic survey

Reflectivity modeling was conducted in advance of the 1997 seismic-reflection survey to assess the potential reflectivity of the local geology (Hajnal and Pandit 1987). The geologic model was based on unpublished borehole geologic picks and structural projections. The velocity properties of the sandstone units were estimated from sonic log data from Rumple Lake (>200 km to the east, Fig. 2), as it was the only sonic log available in the basin at the time. The predicted near surface generated noise was clearly documented by the synthetic shot record (Fig. 13). However, basement reflections appeared visible on the far-offset traces. A synthetic zero-offset reflection section that simulates a final processed seismic image was also determined incorporating

Fig. 10. (*a*) A 32 km long, high-resolution seismic profile S2D (Fig. 2) obtained as a part of a Lithoprobe–industry collaboration. UC, sandstone–basement unconformity; RB, reflection in the exposed basement. The later, mainly east-dipping thrusts reactivated and fragmented the earlier ductile folds, leading to prominently west-dipping blocks. The change in seismic fabric, in the central part of the section (red colour) is interpreted as the seismic marker for the eastern margin of Wollaston–Mudjatic Transition Zone (WMTZ). (*b*) Enlarged example of the seismic image of the unconformity and the associated fault system that extends from the basement into the overlying sandstone.

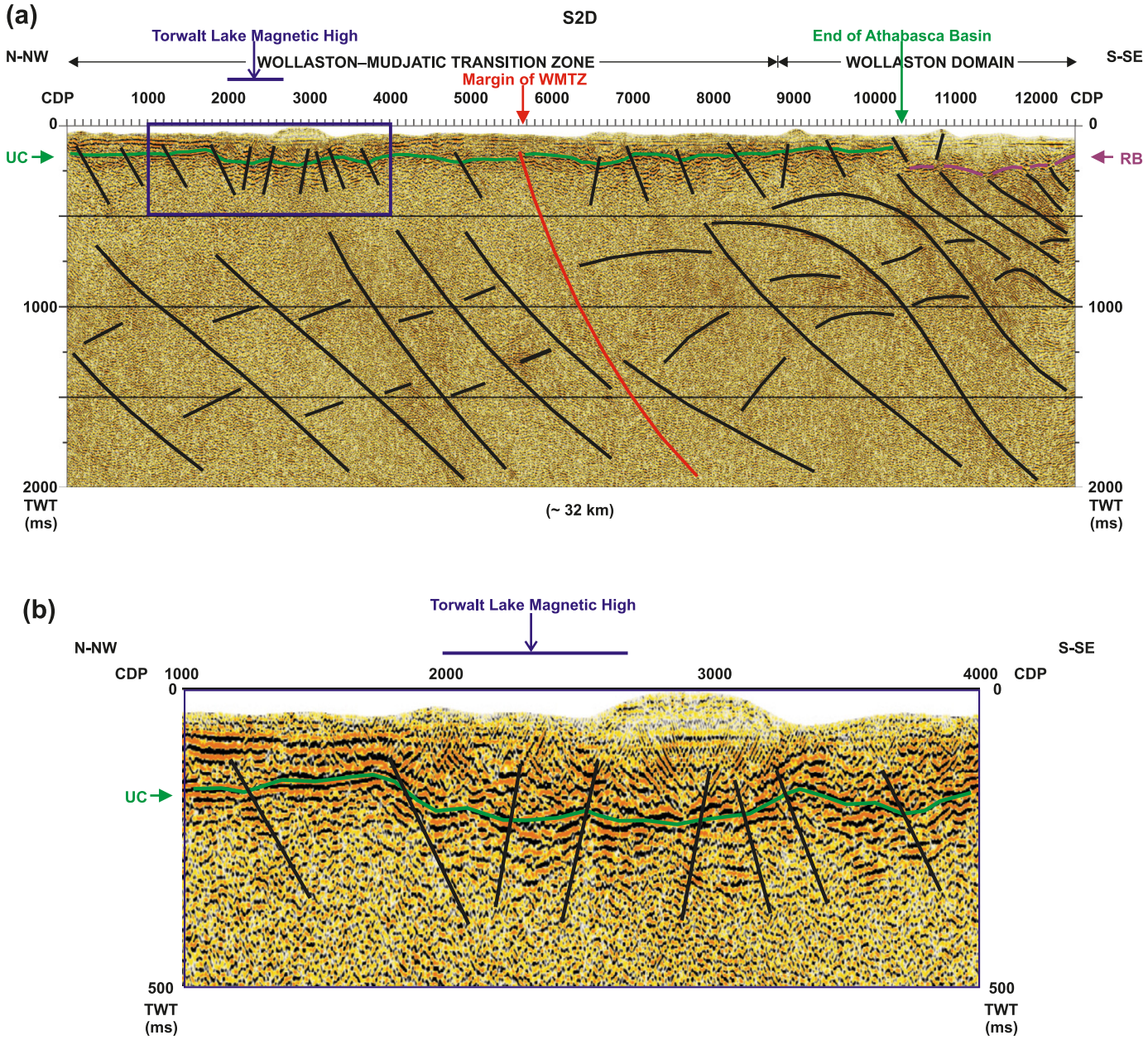

all of the geological data available at the time for the Shea Creek camp. The resultant section shown in Fig. 14 demonstrates the potential of seismic imaging in the area.

More recently, geophysical logs have been acquired at the Shea Creek mine site (Mwenifumbo et al. 2004). Logs for borehole SHE105 are shown in Fig. 12. There is little direct correlation between the log values and the individual formations of the Athabasca Group sandstones (LL-MFc in Fig. 12). However, the velocity log and accompanying acoustic impedance show significant variations over this same interval and a good correlation with the fracture density log. Two thin zones of massive ore are located above (696.2–700.7 m) and below (717–723 m) the unconformity in this borehole in a depth interval characterized by high fracture density and low acoustic impedance values. The lower ore zone is associated with the R3 structure. The synthetic seismic response calculated for the acoustic impedance shows a prominent reflection occurring at the base of the sandstone column.

In the late winter of 1997, the first fully industry-sponsored seismic survey in the basin was conducted south of the Carswell structure (Fig. 2) in the Shea Creek area ~15 km south of the Cluff Lake mine. The locations of the survey lines are shown in Fig. 11. The objectives of the pro-

Fig. 11. (*a*) Location of the Shea Creek project (No. 3 under 2-D seismic in Fig. 2). The Colette and Anne ore bodies were not yet established at the time of the seismic survey in 1997. (*b*) A geologic cross section from Rippert et al. (2000) constructed after the completion of a phase of the drilling program.

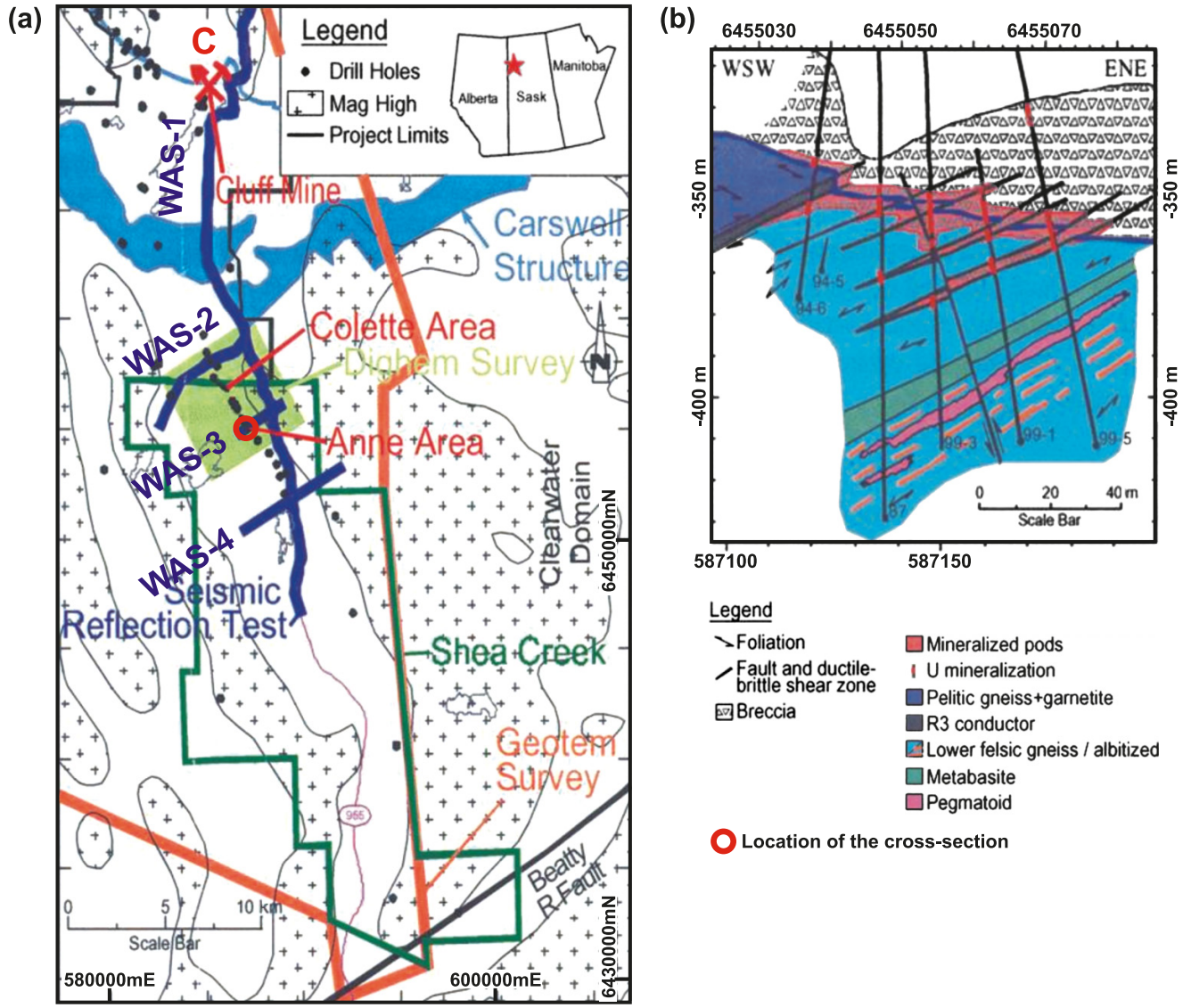

gram included (1) to establish the conditions under which seismic reflection techniques can be effectively used for exploration in this geological setting; (2) to map the unconformity where its depth is variable from ~750 m at the south end of the area to >1200 m close to Cluff Lake; (3) to image the lithostratigraphic and structural variations within the underlying basement complex. The field program included four lines: a long central line (WAS-1) and three shorter cross lines (WAS-2, 3, and 4) located within the area of main exploration interest. A seismic-based interpretation and analysis (described below) were reported to the industrial partner in the fall of 1997. The subsequent drilling program (Fig. 11*b*) confirmed the seismic interpretation (Rippert et al. 2000), and further drilling has outlined the Anne and Collette ore zones and more recently the Kianna deposit (Fig. 11*a*) between the two known mineralized locations (Nimeck and Koch 2008). Following on from this work, the design of a proprietary 3-D seismic survey is in progress to delineate the full extent of the ore zone and establish the comprehensive structural framework of the subsurface.

Interpretation

Interpreted seismic sections for the WAS-1 and WAS-2 profiles are shown in Fig. 15. The unconformity has been traced throughout the area using constraints from nearby boreholes and ensuring consistency at the intersection of the cross lines and WAS-1. Comparison of the depth with unconformity from seismic with borehole depths shows agreement to within ±10 m. The depth of the unconformity increases from ~650 m at the south end of the WAS-1 profile to ~900 m at CDP 6000 (~14.4 km), reaching ~1450 m, 5 km further northward within the deepest region of the annulus of the impact crater. Locations where the unconformity reflection is weaker mainly represent structural lows suggesting that the unconformity surface is controlled

Fig. 12. Logs for SHE105 (after Mwenifumbo et al. 2004). The acoustic impedance (far right) is calculated from the density and velocity logs. Also shown is a synthetic seismic response calculated for the acoustic impedance. OB, overburden; LL, Locker Lake; WPb, Wolverine Point b; WPa, Wolverine Point a; LzL, Lazenby Lake; MFd, Manitou Falls d; MFc, Manitou Falls c; Bsmt, basement.

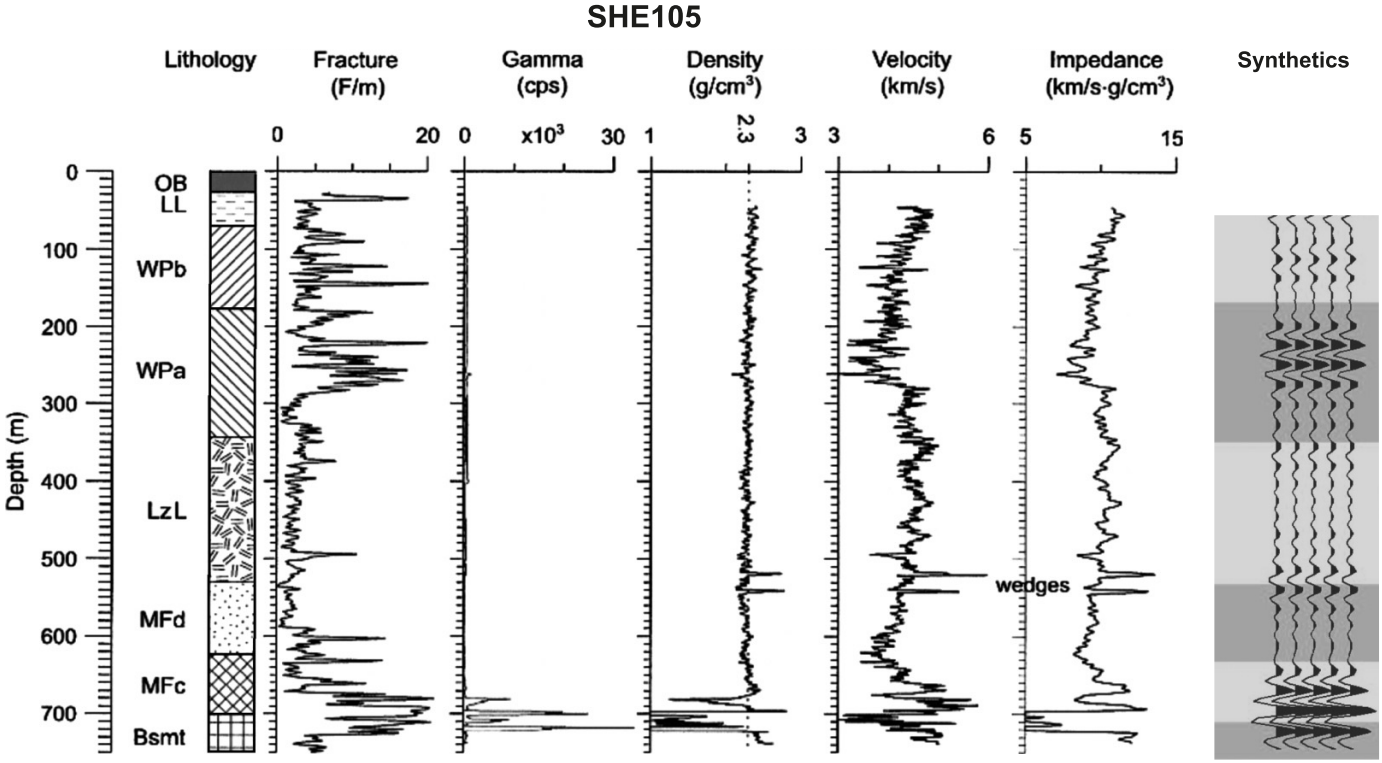

Fig. 13. A synthetic shot record obtained by modeling the geology from borehole SHE08 at Shea Creek. Sandstone velocities were estimated using comparable sandstone units from a Rumple Lake borehole where a sonic log was available (see Fig. 2 for location). The low-frequency coherent noise arrivals dominate the record, reflection energy visible only on the far offset traces. The shot record was generated using the full-waveform reflectivity method.

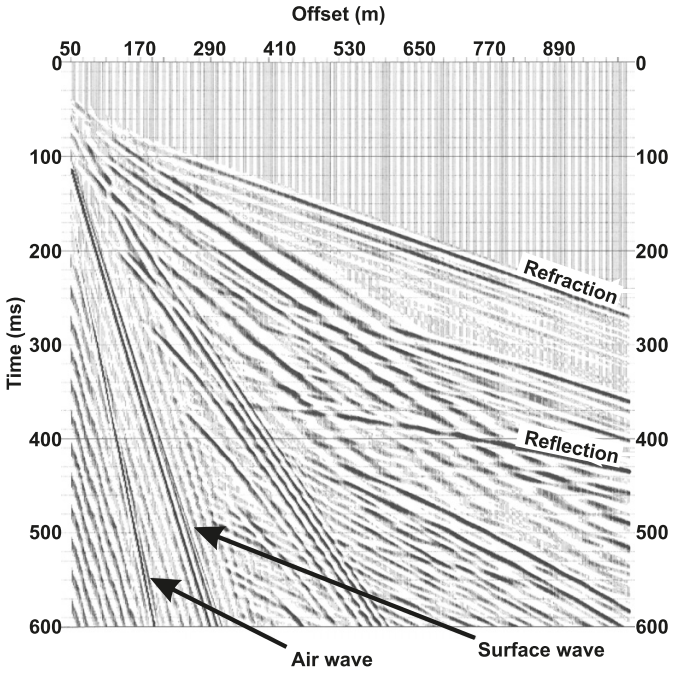

by variable levels of upward thrusting of major basement blocks. Abrupt offsets in the unconformity are generally inferred to be locations of steeply dipping faults along which the hanging walls subsided at later stages of the meteor impact process (Grieve and Masaitis 1994). An exception to this is an unconformity offset near the SHE105 borehole that indicates a reverse fault. The feature was later recognized by drilling as a reverse fault associated with the R3 structure (Nimeck and Koch 2008). Through visual correlation, the interpreted structure can be followed onto the other cross lines (red line Fig. 16). The location of the red line is in agreement with the position of Saskatoon Lake Conductor as defined by Nimeck and Koch (2008).

The subunconformity basement is comparable on all four seismic lines (Fig. 15). Gently south-southwest-dipping reflections evident below the unconformity are interpreted as a part of a prominent upper crustal shear zone with increasing thickness to the west. All the sections show that the shear zone is limited to <3000 m depth within the investigated region. Laterally abrupt terminations of reflectivity are interpreted as steeply dipping fracture zones. These steeply dipping ring-fault systems are characteristics of the basement of the inner region of impact craters (Scott and Hajnal 1988; Hajnal and Scott 1988). The change in dip of these faults, around CDP 2400 on WAS-1 (Fig. 15), is an indication of the outer depth limit of the impact structure. These near vertical faults represent the latest brittle tectonic event in the subsurface, post-dating the gently dipping crustal shear zone. Below ~3000 m, remnants of the early ductile deformation are recognized on the profiles as a gently undulating pattern of reflectivity. It is difficult to ascribe

Fig. 14. Zero-offset synthetic seismic section considering only noise-free arrivals and the geology from eight boreholes along the vicinity of line WAS-1. The faults are located following projections by geologic data. The section was calculated by including only primary reflections (Sheriff and Geldart 2006).

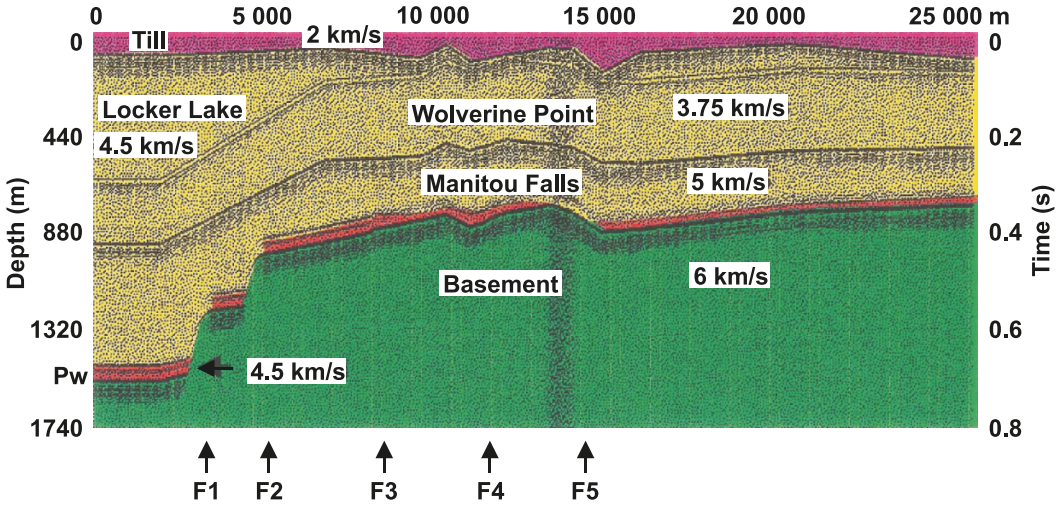

these prominent deeper structures to specific tectonic events, as the regional tectonic framework is not well established here. However, it is recognized that the Lloyd domain is Archean in age, and it was deformed during the Thelon–Talston orogeny (ca. 2.0–1.9 Ga) and later affected by Trans-Hudson orogeny (Rippert et al. 2000). Gibb et al. (1983) postulated that the Clearwater Domain represents a cryptic suture.

McArthur River mine study

High-resolution seismic data were acquired at the McArthur River mining camp in 2001 under the auspices of the EXTECH-IV project (Jefferson and Delaney 2007). A primary objective of this program was to develop new or improved exploration methods and tools for deeply buried unconformity – associated uranium deposits. The seismic program included acquisition of two regional deep sounding seismic profiles, two high-resolution seismic profiles, as well as a pseudo-3-D survey and a vertical seismic profile (VSP) program. Locations of the various seismic components are shown in Fig. 17 and further details of the surveys can be found in Hajnal et al. (2007), White et al. (2007), and Gyorfi et al. (2007).

High-resolution 2-D surveys

The detailed interpretation of lines 12 and 14 from Gyorfi et al. (2007) is superposed on the migrated seismic data in Fig. 18. The unconformity (or unconformity zone) is readily identified on the seismic images in Fig. 18 as a subhorizontal zone of variable reflectivity that separates low reflectivity (sandstone) above from underlying reflections that are predominantly dipping to the southeast. The highly variable nature of the unconformity reflectivity was discussed in the "Acoustic properties" section showing examples from profile 12. In the vicinity of the ore-related P2 structure, the seismic images show a zone of diffuse reflectivity consistent with the complex structural disruption in this zone.

The seismic signature in the overlying sandstone is variable both vertically and laterally. In general, there are no marked differences in seismic facies associated with the individual sandstone members consistent with the conclusions from the geophysical borehole logs (see "Acoustic properties" section). However, stratigraphic information from nearby drill holes together with interpreted basement structural elements provides a consistent framework to correlate markers throughout the sandstone section as portrayed in Fig. 18. Within the basement, southeast-dipping zones of distinct seismic reflectivity and transparency have been interpreted as Wollaston Group metasediments and Archean gneisses, respectively. No boreholes penetrate these deeper parts of the basement, but the polyphase, ductilely deformed and highly metamorphosed properties of these rocks are recognized.

Mainly brittle reverse faults, transecting the Athabasca Group and extending into the basement, are identified on both sections. Borehole RL-68 provides some estimation for calibration of the level of involvement of the structural elements. In this hole, the cumulative vertical offset of the basement is 45 m; and based on the available velocity, the offsets represent 20 ms TWT. Consequently, this observation suggests that the multiple and contrasting dip domains observed within the strata are also indicative of a high level of structural changes. The structural style of the basement on line 14 is further complicated by the apparently high-angle, west-dipping structural features that are not evident on line 12.

Pseudo-3-D survey

An attempt was made to utilize the 2-D survey lines as the basis for forming a low-fold 3-D (or pseudo-3-D) survey. 3-D seismic acquisition was conducted over an area covering $\sim$2.5 km $\times$ 2.0 km in an effort to image the central region of the McArthur River Mining camp (Fig. 17) where the known ore bodies are located. The complexity of the survey layout resulted from restricted access in the camp due to mine buildings and infrastructure. Data acquisition was conducted along an irregular set of source and receiver lines. The receiver lines included the two high-resolution lines (lines 12 and 14) primarily supplemented by receivers along two orthogonal lines. Similarly, source points were lo-

Fig. 15. Final interpreted migrated seismic sections for two (WAS-1 and WAS-2) of the four seismic lines at Shea Creek. Thin, vertical lines and their depth extent indicate the level of tie on the unconformity between the borehole and seismic data. The longer two sections reveal two deformation structures: the younger southwest-dipping thrust zones (SZ) and in greater depth, the older mainly ductile deformation. The steeply dipping line segments mark the ring-fault systems associated with the impact structure.

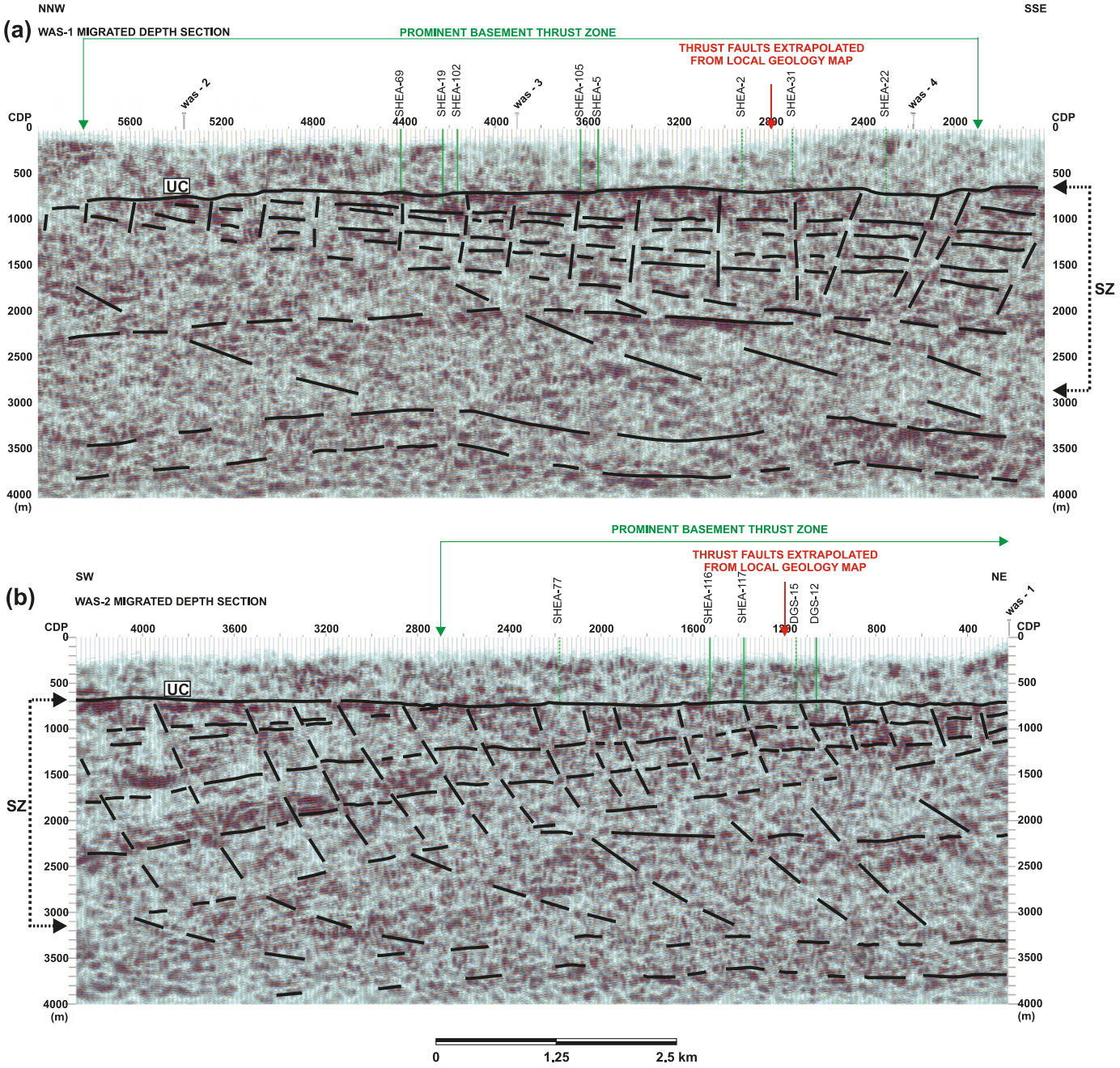

cated along lines 12 and 14, supplemented by several shorter parallel line segments in between. A total of 1500 stationary receiver stations recorded shots from 522 source stations. This limited geometry resulted in a low-fold, irregularly sampled 3-D data volume. The distribution of the data acquisition points permitted an eventual 10 m × 10 m binning of the dataset with resultant fold values ranging mainly from 20 to 50. In spite of these limitations, usable images were obtained in the central part of the region. Details of the 3-D implementation are described in Gyorfi (2006).

The intent of the 3-D survey was to provide areal constraints on the structural framework in the vicinity of the P2 fault and the associated ore zones. A total of 71 boreholes extending to the depth of the unconformity in this central area provide very detailed geological information but are tightly focused on the central exploration trend defined by the EM conductor. The interpretation of the 3-D volume provides a time structure map of the unconformity. Using an average sandstone velocity of 4496 m/s to convert the 3-D seismic volume from time to depth, the estimated error in

Fig. 16. A detailed illustration of the Shea Creek portion of the seismic lines is combined with the locations of the boreholes from the area. The green and yellow marks in the central part outline the R3 conductor as defined by drilling. The red dashed line is a projection of the structure based on seismic images. The green dashed line is the westerly limit of the prominent thrust zone, reaching the unconformity, as defined by the four seismic lines.

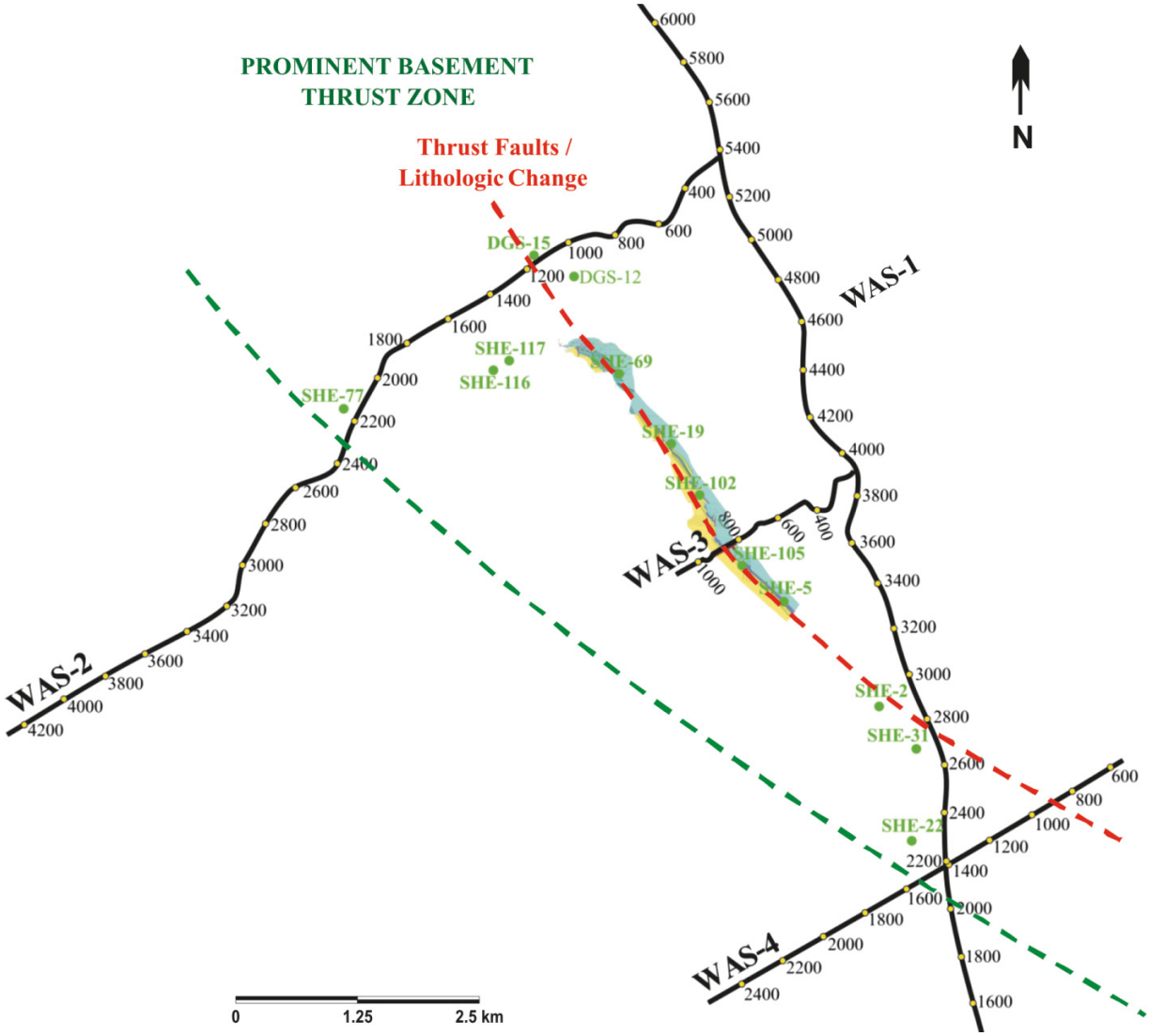

the resultant depth to the unconformity is <4%. Vertical offsets were assigned to six fault segments that were distinguished along the P2 main structural trend.

The final time structure map of the unconformity (Fig. 19*a*) reveals three major structural domains. In the central part, a prominent basement high, oriented northeast–southwest is flanked by two structural lows. In addition, unconformity depths varied within these major units. Outside of the P2 main trend, the variations appeared important on the map, but in absolute value they rarely exceeded several milliseconds. It is clearly evident that the unconformity depth is controlled by a subtle and complicated network of brittle faults. There are three dominant fault directions: northeast–southwest (P2 trend), WNW–ESE, and NNE–SSW. All of the recognized brittle structural elements are characterized by reverse kinematics. The fault dips are variable ranging from medium to subvertical.

The spatial variation on the unconformity surface, its relationship with the intricate fault systems, and most importantly the relationship of the ore pods to the structural environment around them is portrayed in Fig. 19*b*. The reverse faults form a flower structure system above the major P2 fracture zone. The ore pods are located at the intersection(s) of the different fracture zones. The unconformity surface trends with local highs and lows were directly comparable to the production based maps within a few meters of accuracy.

Velocity field

The large maximum source-receiver offsets (~10 000 m) utilized for data acquisition along the regional profiles (A and B in Fig. 17) provided enough depth penetration of refracted arrivals to image velocity variations within the sandstone column and underlying basement. The resultant

Fig. 17. Survey map of the McArthur River program. The investigation includes two longer regional lines (A and B), two 2-D high-resolution profiles (12 and 14) and the pseudo 3-D study within the rectangle. The large dot is the location of the vertical seismic profile (VSP) survey; the small squares are the location of the boreholes along the projected line of the basement conductor.

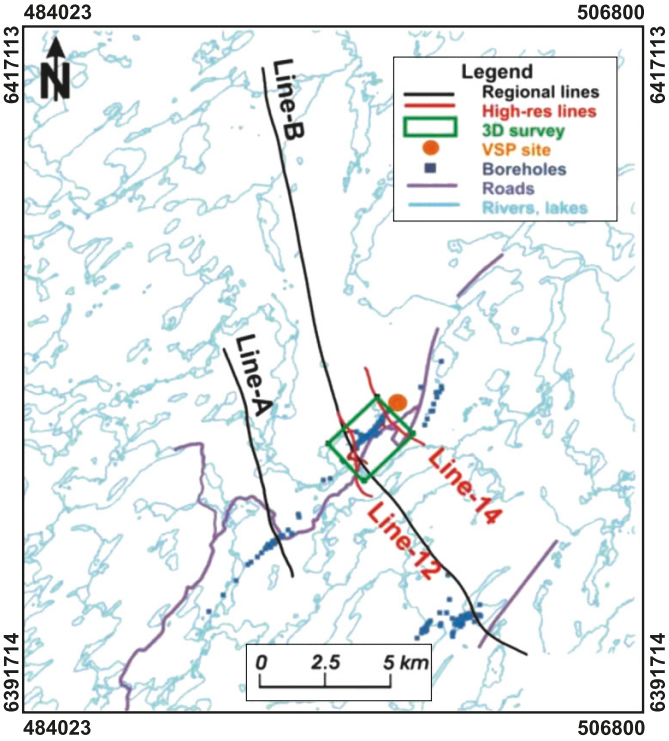

velocity image is shown in Fig. 20. The dark-coloured near-surface velocities (<2000 m/s) outline the glacial till cover along seismic line B. This Quaternary cover is generally thin with local abrupt increases in thickness. Below these anomalous packets of near surface cover, there are significant variations in the velocities determined for the sandstone. The origin of these anomalies, below the seismic line, was investigated in nearby boreholes (Mwenifumbo et al. 2002), revealing that velocity and density are changing in the mineralogically uniform sandstone. Velocity decreases are attributable to increases in fracture density and an associated increase in porosity, whereas velocity and density increases are associated with a decrease in porosity due to silicification. In view of these observations, the local velocity highs are interpreted as zones of intense silicification. Alteration within the sandstone is well documented in the region of the McArthur ore zone (McGill et al. 1993).

Of particular note is a prominent southeast-dipping high-velocity zone (Fig. 20) that occurs near the intersection of the seismic line and the surface projection of the ore-related P2 thrust fault zone. The high velocities extend from the basement into the overlying sandstone column in the hanging wall segment of the fault zone. A comparable velocity anomaly is also observed in the sonic log of a nearby borehole (Gyorfi 2006). Increased velocities associated with silicification of the sandstone has been identified in core measurements (White et al. 2007) and documented in detail along the 2 km strike length of the P2 conductive fault zone (McGill et al. 1993). Within the area of highest velocity values, depletion of clay content at shallow depth, rapid increase of uranium content from 1 ppm to 3–10 ppm, and distinct increase in boron content with depth are also recognized. Alteration zones above the uranium mineralization are a distinct signature of all known unconformity deposits in the basin (Jefferson et al. 2007). This suggests that seismically detected velocity anomalies provide a direct indicator for prospective locations of mineralization at depth. The combination of imaging a prominent basement fault zone and a seismically detected velocity alteration halo above the structure should be considered as a primary indicator for choosing exploration drilling targets in the basin.

Conclusions

The 1994 Lithoprobe Trans-Hudson transect seismic surveys successfully defined the regional crustal architecture beneath the eastern Athabasca Basin and demonstrated how high-resolution seismic techniques could be effectively applied for the purposes of uranium exploration within the basin. Following on from this, several research and commercial seismic studies have been conducted, which have further advanced the adaptation of seismic surveys for uranium exploration, particularly as exploration programs migrate into the deeper reaches of the basin. Some of the important conclusions of these studies are summarized as follows:

(1) Reflectivity within the sandstones is generally weak, being associated primarily with variations in fracture density, porosity, and degree of silicification. In this regard, the seismic images provide limited information about the internal nature of the basin-fill sediments that is directly useful for uranium exploration. However, the effect on reflectivity of the degree and type of alteration (clay–silicification) within the sandstones has not been extensively studied and likely warrants further work.

(2) The lithologic complexity and structural disruption of the basement unconformity and associated regolith result in an associated seismic signature that is highly variable but generally easily identified across the region. As a result, fault offsets of the unconformity, a key exploration target, are readily identified in the seismic images. Further understanding of the properties of the unconformity–regolith and the associated seismic response may allow more geological detail to be determined from the seismic data.

(3) In both case histories (Shea Creek and McArthur River), seismic imaging identifies large-scale shear zones that appear to be directly associated with the known ore-deposits. In the case of Shea Creek, the mineralized band is associated with an anomalous thrust fault within the larger shear zone. This association of the ore deposits with deep-seated faults is consistent with the prodigious volumes of fluid that must be circulated to account for the deposition of the high-grade uranium deposits that characterize the basin (Ingebritsen et al. 2006). All of the deposits that have been seismically investigated are associated with reactivated tectonic domains that were originally deformed during convergence-related processes at the margin of the Trans-Hudson Orogen.

Fig. 18. Interpreted final migrated sections of the high-resolution seismic data for (a) line 12; and (b) line 14, after Gyorfi et al. (2007). The interpretive sections illustrate the spatial structural variation in the vicinity of the ore body and the P2 shear zone.

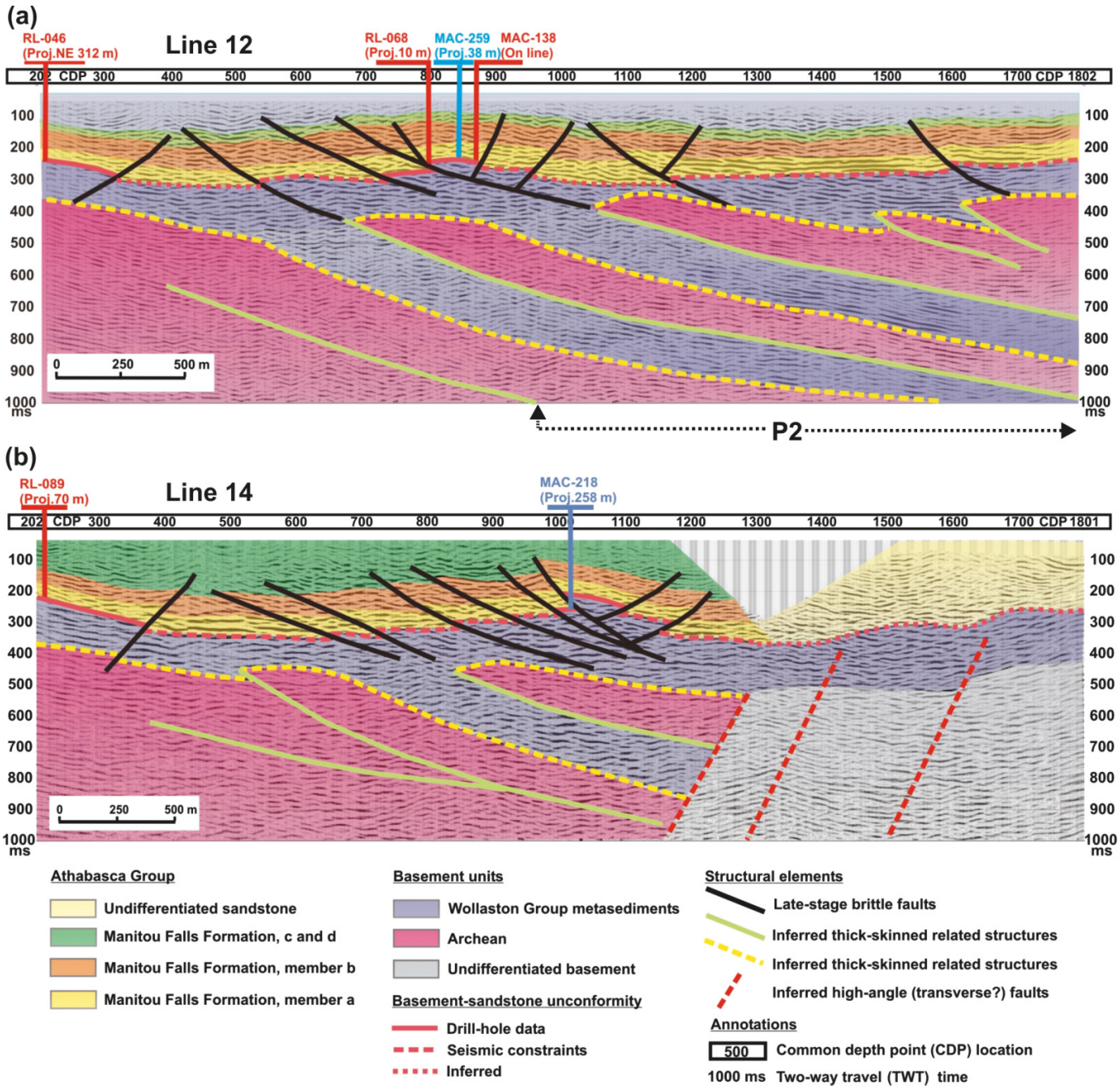

(4) At McArthur River, in addition to the direct connection between the mineralized P2 ore zone and a deep crustal major shear zone, an accompanying high-velocity (silicified) alteration zone is imaged that continues from the basement, across the unconformity, and into the overlying sandstone column. This suggests that the spatial coincidence of seismically imaged high-velocity zones and deep-seated faults that offset the unconformity may be a more broadly applicable exploration targeting tool.

(5) The pseudo-3-D seismic survey of the P2 mineralized zone at McArthur River provided a detailed structural map of the unconformity surface, which included six fault segments with three dominant strike directions, illustrating the complex structural environment in the vicinity of the ore deposit. Although there is an abundance of boreholes in the area, their focused spatial distribution produced only a limited portrayal of the structural environment. The usefulness of this kind of information is demonstrated by the latest 3-D seismic survey at the Millennium ore deposit (Wood et al. 2009) whose primary objective is to map the unconformity surface to identify the best locations for planned mining installations.

Fig. 19. (*a*) Time structural map of the unconformity tied to borehole data. The coloured irregular lines mark the intersections of the reverse fault systems with the unconformity. (*b*) Three dimensional GOCAD display of the structural framework of the McArthur River Mine Camp derived from seismic data and tied to all boreholes within the 3-D study area.

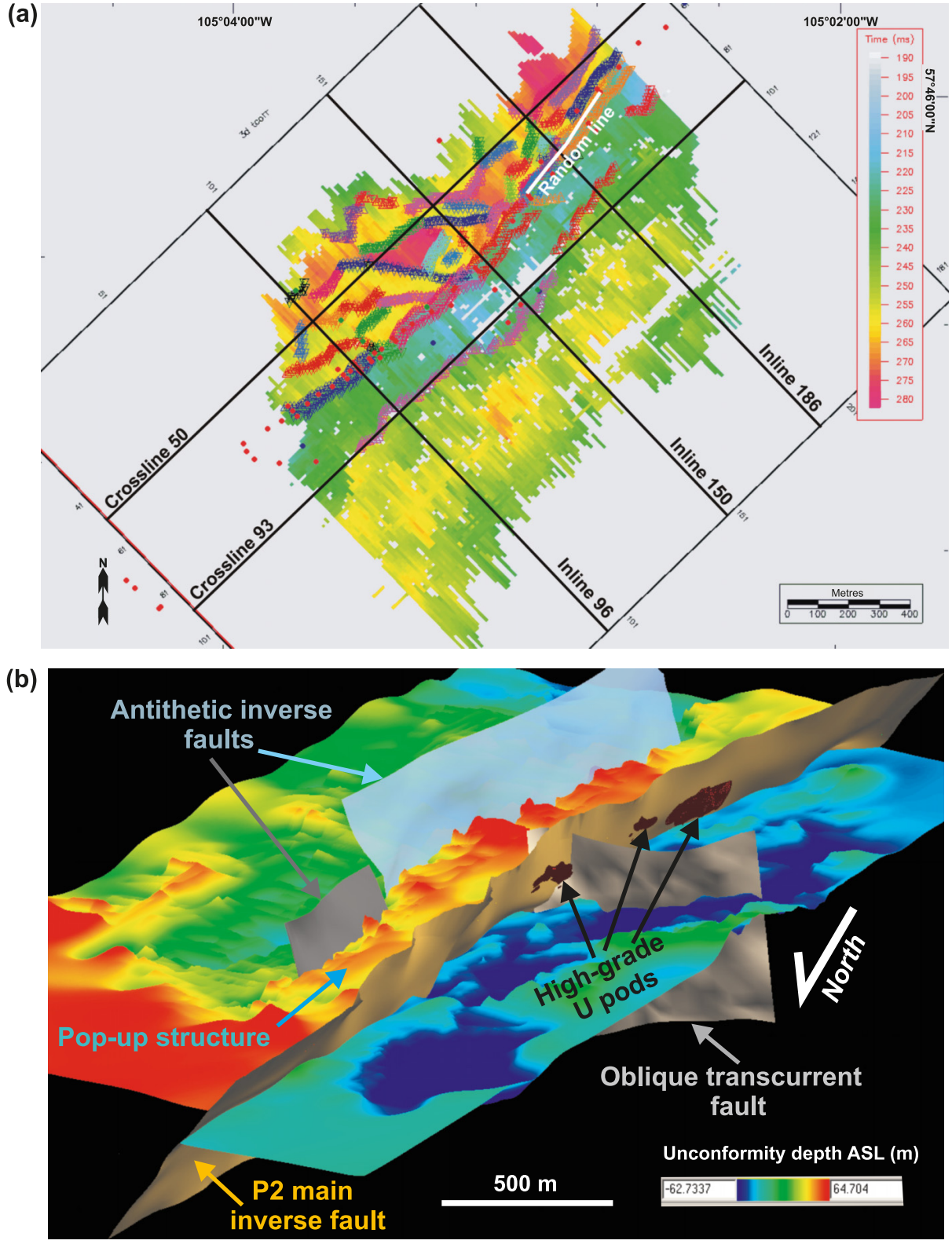

Fig. 20. Interval velocity model along regional line B obtained by tomographic inversion of the first break arrivals. The unconformity was defined by seismic reflections (black line) and borehole data (green vertical lines) with comparable accuracy. Initial generalized linear inversion and a final tomographic inversion were conducted with Hampson-Russell's GLI-3D software.

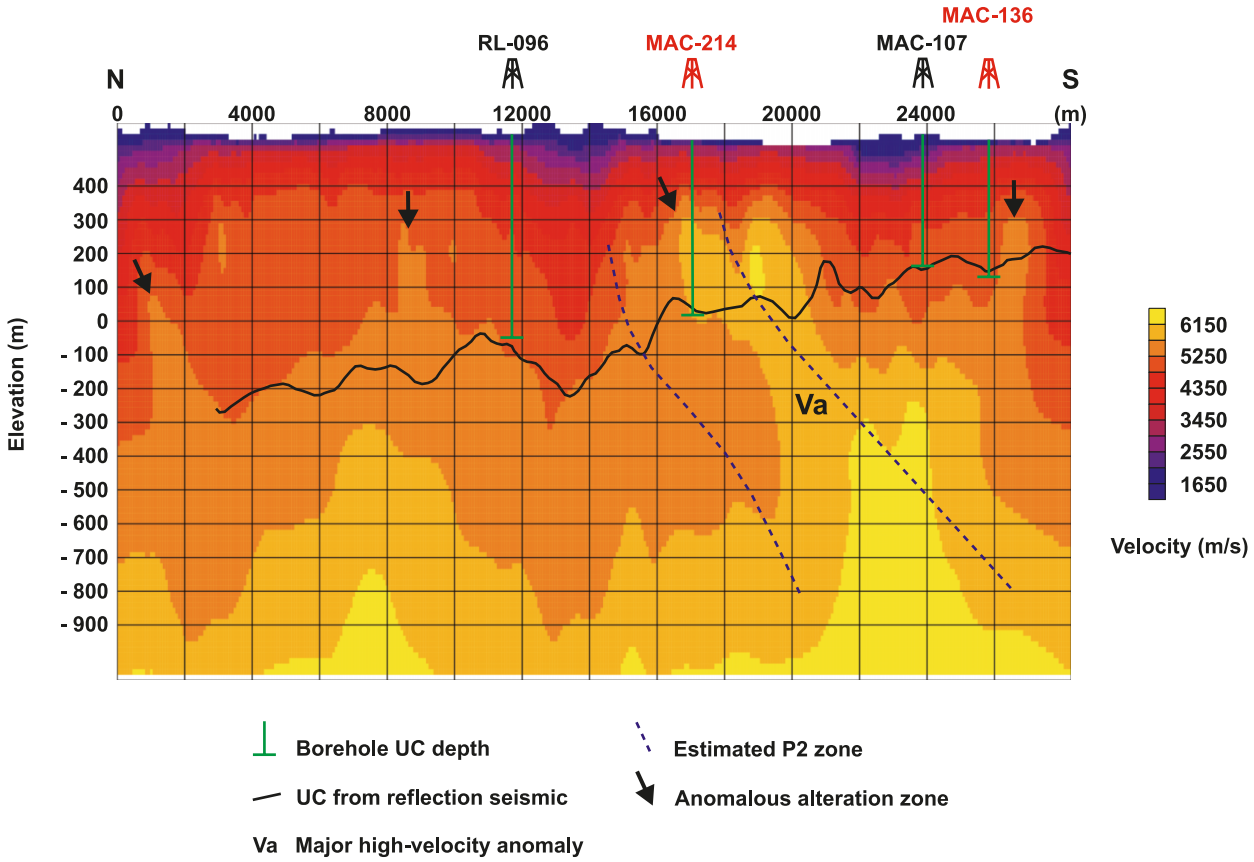

Acknowledgments

Through the years, this investigation benefited from the support of the Natural Sciences and Engineering Research Council of Canada, the Geological Survey of Canada; but more recently contributions by HATHOR, CAMECO, AREVA CORPORATIONS permitted the extensions of limited experiments to broader more effective multifaceted investigations. We thank Landmark Graphics Corp, Schlumberger-GeoQuest-Petrel, OpenSpirit Corporation, and Hampson–Russell Software Services Ltd. for their long-term generous support, permitting us to maintain a current multifaceted software system in our laboratory. The manuscript greatly benefited from the creative suggestions of R. Johnson, the anonymous reviewer, and the Journal Associate Editor R. Clowes.

References

Annesley, I.R., and Madore, C. 2002. Thermotectonics of Archean/Paleoproterozoic basement to the eastern Athabasca unconformity-type uranium deposits. *In* Uranium deposits: from their genesis to their environmental aspects. *Edited by* B. Kribek and J. Zeman. Czech Geological Survey, Prague, Czech Republic. pp. 33–36.

Annesley, I.R., Madore, C., Shi, R., and Krogh, T.E. 1997. U–Pb geochronology of thermotectonic events in the Wollaston Lake area, Wollaston Domain: a summary of 1994–1996 results. Summary of Investigations 1997, Saskatchewan Geological Survey, Saskatchewan Energy and Mines, Miscellaneous Report 97-4, pp. 162–173 (plus map).

Annesley, I.R., Madore, C., Krogh, T.E., Kwok, Y.Y., and Kamo, S.L. 1999. New U–Pb zircon and monazite geochronological results for Archean and Paleoproterozoic basement to the southeastern part of the Athabasca Basin, Saskatchewan. *In* Summary of investigations 1999, Vol. 2. Saskatchewan Geological Survey. Saskatchewan Energy and Mines, Miscellaneous Report 99-4.2, pp. 90–99.

Annesley, I.R., Madore, C., and Portella, P. 2001. Paleoproterozoic structural, metamorphic, and magmatic evolution of the eastern sub-Athabasca basement: Controls on unconformity-type uranium deposits. *In* A hydrothermal odyssey extended conference abstracts, Townsville, Australia, 17–19 May 2001. *Edited by* P.J. Williams. James Cook University EGRU Contribution, Vol. 59, pp. 3–4.

Annesley, I.R., Madore, C., and Hajnal, Z. 2003. Wollaston–Mudjatik transition zone: its characteristics and influence on the genesis of unconformity-type uranium deposits. *In* International conference uranium geochemistry 2003, Nancy, France, 13–16 April 2003. *Edited by* M. Cuney. pp. 55–58.

Annesley, I.R., Madore, C., and Portella, P. 2005. Geology and thermotectonic evolution of the western margin of the Trans-Hudson Orogen: evidence from the eastern sub-Athabasca basement, Saskatchewan. Canadian Journal of Earth Sciences, **42**(4): 573–597. doi:10.1139/e05-034.

Baudemont, D., and Fedorowich, J. 1996. Structural control of ura-

nium mineralization at the Dominique-Peter deposit, Saskatchewan, Canada. Economic Geology and the Bulletin of the Society of Economic Geologists, **91**: 855–874.

Card, C.D., Pana, D., Stern, R.A., and Rayner, N. 2007. New insights into the geological history of the basement rocks to the southwestern Athabasca Basin, Saskatchewan and Alberta 2007. *In* EXTECH IV: geology and uranium exploration technology of the Proterozoic Athabasca Basin, Saskatchewan and Alberta. *Edited by* C.W. Jefferson and G. Delaney. Geological Survey of Canada, Bulletin 588 (also Saskatchewan Geological Society, Special Publication 18; Geological Association of Canada, Mineral Deposits Division, Special Publication 4), pp. 119–134.

Cosma, C., and Enescu, N. 2001. Characterization of fractured rock in the vicinity of tunnels by swept impact seismic technique. International Journal of Rock Mechanics and Mining Sciences, **38**(6): 815–821. doi:10.1016/S1365-1609(01)00046-6.

Fouques, J.P., Fowler, M., Knipping, H.D., and Schimman, K. 1986. The Cigar Lake uranium deposit: discovery and general characteristics. *In* Uranium deposits of Canada. *Edited by* E.I. Evans. Canadian Institute of Mining and Metallurgy, Special Vol. 33, pp. 218–229.

Gibb, R.A., Thomas, M.D., Lapointe, P.L., and Mukhopadhyay, M. 1983. Geophysics of proposed Proterozoic sutures in Canada. Precambrian Research, **19**(4): 349–384. doi:10.1016/0301-9268(83)90021-9.

Grieve, R.A.F., and Masaitis, V.I. 1994. The economic potential of terrestrial impact craters. International Geology Review, **36**(2): 105–151. doi:10.1080/00206819409465452.

Gyorfi, I. 2006. Seismic constrains on the geological evolution of the McArthur River region; in view of the eastern Athabasca Basin, northern Saskatchewan, Ph.D. thesis, University of Saskatchewan, Saskatoon, Sask.

Gyorfi, I., Hajnal, Z., White, D.J., Takacs, E., Reilkoff, B., Annesley, I., Powell, B., and Koch, R. 2007. High resolution seismic survey from the McArthur River region: contributions to mapping of the complex P2 uranium ore zone, Athabasca Basin, Saskatchewan. *In* EXTECH IV: geology and uranium exploration technology of the Proterozoic Athabasca Basin, Saskatchewan and Alberta. *Edited by* C.W. Jefferson and G. Delaney. Geological Survey of Canada, Bulletin 588 (also Saskatchewan Geological Society, Special Publication 18; Geological Association of Canada, Mineral Deposits Division, Special Publication 4), pp. 397–412.

Hajnal, Z., and Pandit, B. 1987. Practical application of reflectivity method. Canadian Journal of Exploration Geophysics, **24**: 101–109.

Hajnal, Z., Stauffer, M.R., and King, M.S. 1983. Petrophysics of the Athabasca basin near the Midwest Lake uranium deposit. *In* Uranium exploration in Athabasca basin Saskatchewan, Canada. *Edited by* E.M. Cameron. Geological Survey of Canada, Paper 82-11, pp. 303–310.

Hajnal, Z., and Scott, D. 1988. Reflection study of the Haughton impact crater. Journal of Geophysical Research, **93**(B10): 11 930 – 11 942. doi:10.1029/JB093iB10p11930.

Hajnal, Z., Lucas, S., White, D., Bezdan, S., Stauffer, M.R., and Thomas, M.T. 1996. Seismic reflection images of high-angle faults and linked detachments in the Trans-Hudson Orogen. Tectonics, **15**: 427–439. doi:10.1029/95TC02710.

Hajnal, Z., Annesley, I.R., White, D., Matthew, R.B., Sopuck, V., Koch, R., Leppin, M., and Ahuja, S. 1997. Sedimentary-hosted mineral deposits: A high-resolution seismic survey in the Athabasca Basin. *In* Proceedings of Exploration 97: 4th Decennial International Conference on Mineral Exploration, Toronto, Ont. *Edited by* A.G. Gubins. GEO/FX, Palo Alto, Calif. pp. 421–432.

Hajnal, Z., Lewry, J., White, D.J., Ashton, K., Clowes, R., Stauffer, M., Gyorfi, I., and Takacs, E. 2005. The Sask craton and Hearne Province margin: seismic reflection studies in the western Trans-Hudson Orogen. Canadian Journal of Earth Sciences, **42**(4): 403–419. doi:10.1139/e05-026.

Hajnal, Z., Takacs, E., White, D.J., Gyorfi, I., Powell, B., and Koch, R. 2007. Regional seismic signature of the basement and crust beneath the McArthur River mine district, Athabasca Basin, Saskatchewan. *In* EXTECH IV: geology and uranium exploration technology of the Proterozoic Athabasca Basin, Saskatchewan and Alberta. *Edited by* C.W. Jefferson and G. Delaney. Geological Survey of Canada, Bulletin 588 (also Saskatchewan Geological Society, Special Publication 18; Geological Association of Canada, Mineral Deposits Division, Special Publication 4), pp. 389–395.

Hajnal, Z., Pandit, B., Annesley, I., White, D.J., Reilkoff, B., McCready, A., and Wallster, D. 2009. Complex seismic signatures of the Athabasca basin subsurface. *In* 2009 Joint Assembly (AGU, CGU, GAC, MAC, MSA, IAH-CNC), 24–25 May 2009, Toronto, Ont., S31A-19.

Hobson, G.D., and MacAuley, H.A. 1969. A seismic reconnaissance survey of the Athabaca formation, Alberta and Saskatchewan, Geological Survey of Canada, Paper 69-18, pp. 35–47.

Ingebritsen, S., Sanford, W., and Neuzil, C. 2006. Groundwater in geological processes. 2nd ed. Cambridge University Press, Cambridge, UK.

Jefferson, C.W., and Delaney, G. 2007. EXTECH IV: geology and uranium exploration technology of the Proterozoic Athabasca Basin, Saskatchewan and Alberta. Geological Survey of Canada, Bulletin 588 (also Saskatchewan Geological Society, Special Publication 18; Geological Association of Canada, Mineral Deposits Division, Special Publication 4), p. 644.

Jefferson, C.W., Thomas, D.J., Gandhi, S.S., Remaekers, P., Delaney, G., Brisbin, D., et al. 2007. Unconformity-associated uranium deposits of the Athabasca Basin, Saskatchewan and Alberta. *In* EXTECH IV: geology and uranium exploration technology of the Proterozoic Athabasca Basin, Saskatchewan and Alberta. *Edited by* C.W. Jefferson and G. Delaney. Geological Society of Canada, Bulletin 588 (also Saslatcjewam Geological Society, Special Publication 18; Geological Association of Canada, Mineral Deposits Division, Special Publication 4), pp. 23–68.

Mandler, H.A.F., and Clowes, R.M. 1997. Evidence for extensive tabular intrusions in the Precambrian shield of western Canada: A 160-km-long sequence of bright reflections. Geology, **25**(3): 271–274. doi:10.1130/0091-7613(1997)025<0271:EFETII>2.3.CO;2.

McGill, B.D., Marlatt, J.L., Matthews, R.B., Sopuck, V.J., Homeniuk, L.A., and Hubregtse, J.J. 1993. The P2 North Uranium deposit, Saskatchewan, Canada. Exploration and Mining Geology, **2**: 321–331.

Mwenifumbo, C.J., Elliot, B.E., Drever, G., and Wood, G. 2002. Borehole geophysical logging of two deep surface boreholes and one underground borehole at McArthur River. *In* Summary of Investigations 2002, Vol. 2. Saskatchewan Geological Survey, Saskatchewan Industry and Resources, Miscellaneous Report 2002-2-4.1, pp. 1–9.

Mwenifumbo, C.J., Elliott, B.E., Jefferson, C.W., Bernius, G.R., and Pflug, K.A. 2004. Physical rock properties from the Athabasca Group: designing geophysical exploration models for unconformity uranium deposits. Journal of Applied Geophysics, **55**(1–2): 117–135. doi:10.1016/j.jappgeo.2003.06.008.

Nimeck, G., and Koch, R. 2008. A progressive geophysical ex-

ploration strategy at the Shea Creek uranium deposit. Leading Edge (Tulsa, Okla.), **27**(1): 52–63. doi:10.1190/1.2831680.

Overton, A. 1977. Seismic determination of basement depths, Athabasca basin, Geological Survey of Canada, Report. of Activities Part C, Paper 77-1C, p. 1925.

Pagel, M., and Svab, M. 1985. Petrographic and geochemical variations within the Carswell structure metamorphic core and their implications with respect to uranium mineralization. Geological Assocication of Canada, **29**: 1–18.

Portella, P., and Annesley, I.R. 2000. Paleoproterozoic thermotectonic evolution of the eastern sub-Athabasca basement, northern Saskatchewan: Integrated geophysical and geological data. *In* Summary of Investigations 2000, Vol. 2. Saskatchewan Geological Survey, Saskatchewan Energy and Mines, Miscellaneous Report 2000-4.2, pp. 191–200.

Rainbird, R.H., Stern, R.A., Rayner, N., and Jefferson, C.W. 2007. Age, provenance and regional correlation of the Athabasca Group, Saskatchewan and Alberta, constrained by igneous and detrital zircon geochronology. *In* EXTECH IV: geology and uranium exploration technology of the Proterozoic Athabasca Basin, Saskatchewan and Alberta. *Edited by* C.W. Jefferson and G. Delaney. Geological Survey of Canada, Bulletin 588 (also Saskatchewan Geological Society, Special Publication 18; Geological Association of Canada, Mineral Deposits Division, Special Publication 4), pp. 193–210.

Ramaekers, P., Jefferson, C.W., Yeo, G.M., Collier, D.G.F., Long, G., Drever, S., et al. 2007. Revised geological map and stratigraphy of the Athabasca Group, Saskatchewan and Alberta. *In* EXTECH IV: geology and uranium exploration technology of the Proterozoic Athabasca Basin, Saskatchewan and Alberta. *Edited by* C.W. Jefferson and G. Delaney. Geological Survey of Canada, Bulletin 588 (also Saskatchewan Geological Society, Special Publication 18; Geological Association of Canada, Mineral Deposits Division, Special Publication 4), pp. 155–192.

Rippert, J.C., Koning, E., Robbins, J., Koch, R., and Baudemont, D. 2000. The Shea Creek uranium project, west Athabasca Basin, Saskatchewan, Canada. *In* GeoCanada 2000, Calgary, Alta., 29 May 29 – 2 June 2000. Abstract 570 [CD-ROM].

Schreiner, B.T. 1983. Quaternary geology of the NEA/IAE test area. *In* Uranium exploration in Athabasca basin, Saskatchewan, Canada. *Edited by* E.M. Cameron. Geological Survey of Canada, Paper 82, pp. 27–32.

Scott, F. 1983. Midwest Lake uranium discovery. *In* Uranium exploration in Athabasca basin, Saskatchewan, Canada. *Edited by* E.M. Cameron. Geological Survey of Canada, Paper 82-11, pp. 41–50.

Scott, D., and Hajnal, Z. 1988. Seismic signature of the Haughton structure. Meteoritics, **23**: 239–247.

Sheriff, R.E., and Geldart, L.P. 2006. Exploration Seismology. 2nd ed. Cambridge University Press, Cambridge, UK.

Tran, H.T., Ansdell, K., Bethune, K., Watters, B., and Ashton, K. 2003. Nd isotope and geochemical constraints on the depositional setting of Paleoproterozoic metasedimentary rocks along the margin of the Archean Hearne craton, Saskatchewan, Canada. Precambrian Research, **123**(1): 1–28. doi:10.1016/S0301-9268(03)00012-3.

White, D.J., Hajnal, Z., Roberts, B., Gyorfi, I., Reilkoff, B., Bellefleur, G., et al. 2007. Seismic methods for uranium: an overview of EXTECH IV seismic studies at the McArthur River mining camp, Athabasca Basin, Saskatchewan. *In* EXTECH IV: geology and uranium exploration technology of the Proterozoic Athabasca Basin, Saskatchewan and Alberta. *Edited by* C.W. Jefferson and G. Delaney. Geological Survey of Canada, Bulletin 588 (also Saskatchewan Geological Society, Special Publication 18; Geological Association of Canada, Mineral Deposits Division, Special Publication 4), pp. 363–388.

Wood, G., O'Dowd, C., Cosma, C., and Enescu, N. 2009. The application of borehole seismic techniques in mine development at the Millennium uranium deposit, Northern Saskatchewan, Canada. International Atomic Energy Agency Proceeding Series, **175**(29): 10–16.

Yordkayhun, S., Ivanova, A., Giese, R., Juhlin, C., and Cosma, C. 2009. Comparison of surface seismic sources, at the CO2 SINK site, Ketzin, Germany. Geophysical Prospecting, **57**(1): 125–139. doi:10.1111/j.1365-2478.2008.00737.x.